TECHNICAL REPORT NO. 71-20

SPECIAL REPORT, VT/0703

ANALYSIS OF DATA FROM SIX PORTABLE STRAINMETERS IN SOUTHERN NEVADA

APPROVED FOR PUBLIC RELEASE
DISTRIBUTION UNLIMITED

TELEDYNE GEOTECH

Security Classification

DOCUMENT CONTROL DATA - R & D

(Security classification of title, body of abstract and indexing annotation must be entered when the overall report is classified)

1 ORIGINATING ACTIVITY (Corporate author)	2a. REPORT SECURITY CLASSIFICATION
Teledyne Geotech 3401 Shiloh Road, Garland, Texas 75041	2b. GROUP

3 REPORT TITLE

Analysis of Data from Six Portable Strainmeters in Southern Nevada

4 DESCRIPTIVE NOTES (Type of report and inclusive dates)

5 AUTHOR(S) (First name, middle initial, last name)

Robert C. Shopland

6 REPORT DATE	7a. TOTAL NO. OF PAGES	7b. NO. OF REFS
31 October 1971	89	7

8a. CONTRACT OR GRANT NO	9a. ORIGINATOR'S REPORT NUMBER(S)
F33657-70-C-0646	
b. PROJECT NO VELA T/0703	Technical Report No. 71-20
c.	9b. OTHER REPORT NO(S) (Any other numbers that may be assigned this report)
d.	

10 DISTRIBUTION STATEMENT

Approved for Public Release.
Distribution Unlimited

11 SUPPLEMENTARY NOTES	12 SPONSORING MILITARY ACTIVITY
	Advanced Research Projects Agency Nuclear Monitoring Research Office 1400 Wilson Blvd., Arlington, Virginia 22209

13 ABSTRACT

This report covers an analysis of secular strains over an annual cycle at six portable strain sites in southern Nevada as well as a study of the strain characteristics of signals from significant events recorded in the time interval 23 January 1970 through 31 July 1971. Measurements of quasi-static strains support the hypothesis that dynamic loading by the seismic waves from explosions and earthquakes trigger a local release of tectonic strain (a strain step). Furthermore, trends in the direction of strain steps appear to be related to regional tectonic strain. On the other hand, residual changes in strain of the order of 1×10^{-5} m/m over an annual cycle do not fit any pattern that would suggest a long-term trend in the regional strain field, but appear to be peculiar to individual sites, or at most to subregions of the area covered by the six sites. Earthquake coupling factors among the six sites show nearly the same relative values as obtained from measurements of tidal coupling. Coupling factors range from a low of approximately 0.2 at both Rawhide Mountain and Oak Spring Butte to 1.0 at Kawich Peak. Low coupling factors at Rawhide Mountain and Oak Spring Butte could be related to the fact that the strainmeter tunnels are located in sharp ridges—the only apparent geological feature that is common to both sites yet is absent at the other four. The simultaneous occurrence of complex short-term and long-term temperature and pressure effects requires complex processing procedures to remove environmentally-induced strains in order to study the decay characteristics of strain steps. In an exceptional case, the strain in the winter season at Rawhide Mountain was predicted within 4×10^{9} m/m over a 3-hour time period following a hypothetical strain step. Data from case studies of NTS events CYATHUS, BANEBERRY, MINIATA, HAREBELL, SHAPER, and a magnitude 4 earthquake near the NTS, and the San Joaquin Valley earthquake, suggest that the rise time of the strain step is more strongly influenced by tectonic conditions at the recording site than by source conditions, at the epicentral distances and the event magnitudes considered.

DD FORM 1 NOV 65 1473

Unclassified
Security Classification

TECHNICAL REPORT NO. 71-20

SPECIAL REPORT, VT/0703

ANALYSIS OF DATA FROM SIX PORTABLE STRAINMETERS IN SOUTHERN NEVADA

by

Robert C. Shopland

Sponsored by

Advanced Research Projects Agency
Nuclear Monitoring Research Office
ARPA Order No. 624

Acknowledgement

This research was supported by the Advanced Research Projects Agency, Nuclear Monitoring Research Office, under Project VELA-Uniform and accomplished under the technical direction of the Air Force Technical Applications Center under Contract No. F33657-70-C-0646.

Approved for Public Release.
Distribution Unlimited.

Teledyne Geotech
3401 Shiloh Road
Garland, Texas

31 October 1971

IDENTIFICATION

AFTAC Project No. VT/0703
Project Title: Long-Range Seismic Measurements
ARPA Order No. 624
ARPA Code No. 8F10
Contractor: Teledyne Geotech
Contract No. F33657-70-C-0646, Amendment 4
Program Manager: R. G. Reakes (214) 271-2561, ext. 230
Garland, Texas 75041

CONTENTS

CONTENTS, Continued

ILLUSTRATIONS

ILLUSTRATIONS, Continued

ILLUSTRATIONS, Continued

ILLUSTRATIONS, Continued

TABLES

ABSTRACT

This report covers an analysis of secular strains over an annual cycle at six portable strain sites in southern Nevada as well as a study of the strain characteristics of signals from significant events recorded in the time interval 23 January 1970 through 31 July 1971. Measurements of quasi-static strains support the hypothesis that dynamic loading by the seismic waves from explosions and earthquakes trigger a local release of tectonic strain (a strain step). Furthermore, trends in the direction of strain steps appear to be related to regional tectonic strain. On the other hand, residual changes in strain of the order of 1×10^{-5} m/m over an annual cycle do not fit any pattern that would suggest a long-term trend in the regional strain field, but appear to be peculiar to individual sites, or at most to subregions of the area covered by the six sites. Earthquake coupling factors among the six sites show nearly the same relative values as obtained from measurements of tidal coupling. Coupling factors range from a low of approximately 0.2 at both Rawhide Mountain and Oak Spring Butte to 1.0 at Kawich Peak. Low coupling factors at Rawhide Mountain and Oak Spring Butte could be related to the fact that the strainmeter tunnels are located in sharp ridges - the only apparent geological feature that is common to both sites yet is absent at the other four. The simultaneous occurrence of complex short-term and long-term temperature and pressure effects requires complex processing procedures to remove environmentally-induced strains in order to study the decay characteristics of strain steps. In an exceptional case, the strain in the winter season at Rawhide Mountain was predicted within 4×10^{9} m/m over a 3-hour time period following a hypothetical strain step. Data from case studies of NTS events CYATHUS, BANEBERRY, MINIATA, HAREBELL, SHAPER, and a magnitude 4 earthquake near the NTS, and the San Joaquin Valley earthquake, suggest that the rise time of the strain step is more strongly influenced by tectonic conditions at the recording site than by source conditions, at the epicentral distances and the event magnitudes considered.

SPECIAL REPORT, VT/0703

ANALYSIS OF DATA FROM SIX PORTABLE STRAINMETERS IN SOUTHERN NEVADA

1. INTRODUCTION

1.1 OBJECTIVES

This is a special report describing the work undertaken in the period 15 August 1970 to 31 August 1971 to operate instruments and analyze data from six portable strainmeter systems at six sites on and near the Nevada Test Site (NTS). The work was performed under Contract F33657-70-C-0646, Amendment 4. The report is submitted in accordance with sequence number A003 of the Contract Data Requirements List. The Statement of Work is included as appendix 1.

Prior to this contract period, the six strainmeters were operated in the period February through April 1970 to evaluate their field operational characteristics and to record the HANDLEY event. The work is described in Technical Report No. 70-10, Special Report, VT/8703, Evaluation of Field Operational Characteristics of the Portable Strainmeter System, dated 31 July 1971.

Following the HANDLEY event, the six systems were removed and stored in a government warehouse at Mercury, Nevada. The strainmeters were left in place in order to preserve temperature stability in the tunnels and trenches.

Operation of the six sites at the locations shown in figure 1 and table 1 was resumed in September 1970 under the present contract. One objective of the operation was to obtain continuous recording of strain and to analyze long-term environmental effects observed during an annual cycle. Specific goals included the following:

a. Measuring both the short-term and long-term strain characteristics at each site;

b. Evaluating the limitations of shallow tunnel and trench sites in terms of strains induced by the tides and temperature changes.

Another objective was to provide detailed interpretations of strain data obtained from significant individual events. Specific goals included the following:

a. The determination of strain characteristics of signals selected by the Project Office;

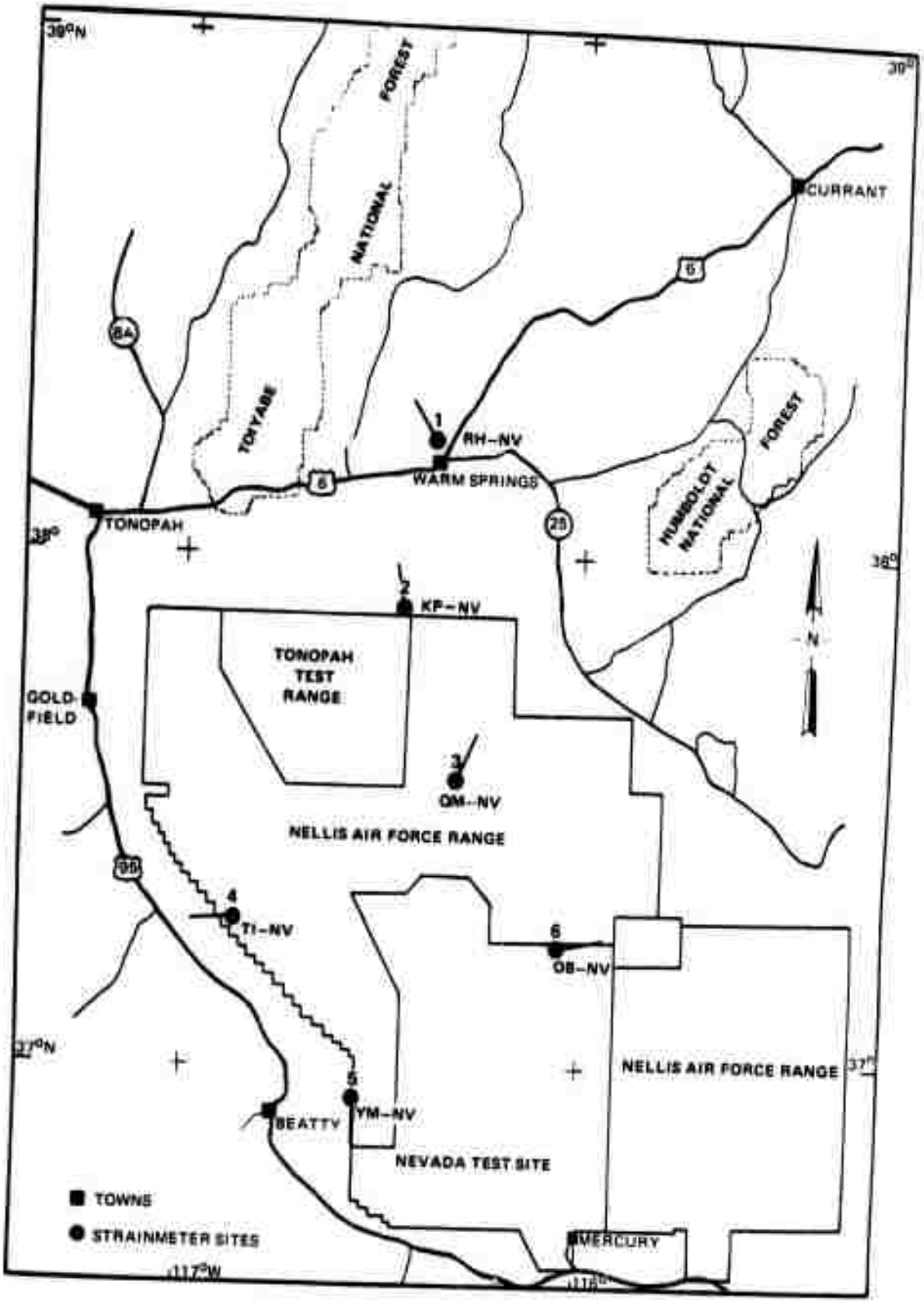

Figure 1. Location of strain sites

G 6542

Table 1. Portable strainmeter site locations

Site No.	Site name	Site designator	Geographic coordinates		Elevation		Approximate azimuthal orientation of strainmeter	Type of site
			N. Lat.	W. Long.	Feet	Meters		
1	Rawhide Mtn., Nevada	RH-NV	38°13'36"	116°22'53"	5800	1768	325°	Tunnel
2	Kawich Peak, Nevada	KP-NV	37°53'51"	116°27'33"	7000	2134	356°	Tunnel
3	Quartzite Mtn., Nevada	QM-NV	37°33'47"	116°19'04"	6160	1878	020°	Tunnel
4	Tolicha Peak, Nevada	TI-NV	37°17'07"	116°52'01"	5000	1524	266.5°	Trench
5	Yucca Mtn., Nevada	YM-NV	36°55'53"	116°33'15"	4400	1341	182.5°	Trench
6	Oak Spring Butte, Nevada	OB-NV	37°14'09"	116°03'09"	5680	1731	081°	Tunnel

b. A study of the dynamic characteristics of the strain signal from earthquakes and explosions - the study, of necessity, would be limited to a case study of one event recorded at several sites, and a limited number of events recorded at one site; and

c. The measurement of site coupling coefficients.

The operation was carried out under the following limitations:

a. The six portable strainmeter systems were maintained by only one man;

b. Few spare parts were kept on hand either in the field or at the contractor's home office;

c. The system was operated without a control circuit to automatically recenter the transducer. An automatic recentering modification, which was recommended following evaluation of field operational characteristics in the spring of 1970, would have prevented secular strains from driving unattended systems beyond their usable range.

Despite these restrictions and obstacles, continuity of recording was sufficient to furnish usable data to the University of Washington (Dr. S. W. Smith and Dr. Rainer Kind) and to the University of Nevada (Dr. Alan Ryall and Dr. Steve Malone). Smith and Kind (1971) have prepared a paper describing changes in the regional secular strain field.

1.2 SYSTEM MODIFICATIONS

Table 2 contains the recording format and a schedule of changes for the portable strain system in the time period March 1970 through July 1971. Following resumption of operation about 1 September 1970 the following modifications were performed:

a. The fuel supply was doubled at each site by the addition of one 100 lb tank of propane and an automatic switching valve. The 30-day fuel supply was necessary to avoid difficulties in the scheduling of visits by the lone operator.

b. The radio circuit was rewired to allow application of a 5-minute manual reference signal at 0.1 Hz to facilitate playback procedures, since automatic time search equipment for IRIG is not available at the playback facility.

c. At the end of September 1970 an interim wide-band low-gain strain channel was added to the system by tapping into the secondary strain channel (No. 5) preceding the 0.01 Hz filter and recording the signal on channel No. 3 of the tape recorder. (See item 3b in table 2).

Table 2. Recording format and schedule of changes

Magnetic Tape Recorder Channel No.		Mode
1	Pri. Strain	FM
2	Pri. Strain Reset Count	Direct
2	Wide-Band Hi-Gain Strain	FM
3	Tube Temp. Reset Count	Direct
3	Wide Band Lo-Gain Strain	Direct
3	Wide Band Lo-Gain Strain	FM
4	Tube Temp	FM
5	Sec. Strain	FM
6	Environmental	FM
7	Time Code (WWVB)	Direct

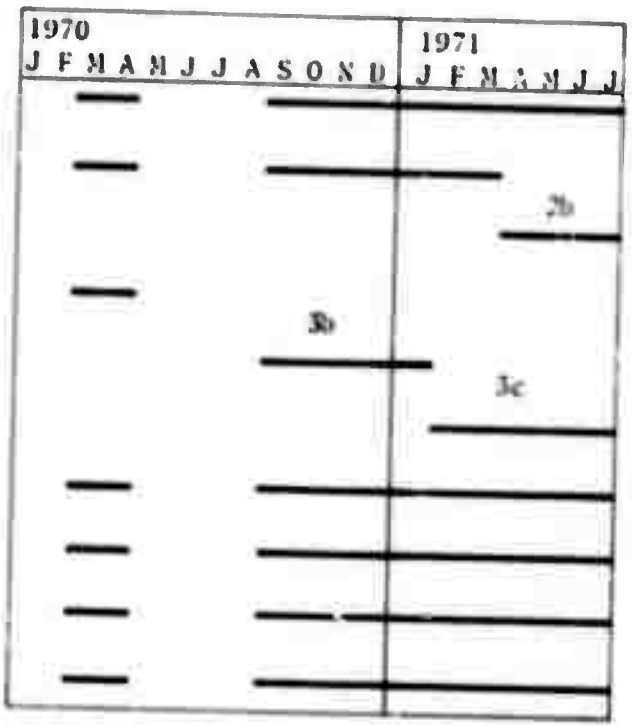

Site	(3b) Installed wide-band lo-gain strain in channel No. 3, direct mode, 0.09 - 5 Hz	(3c) Converted channel No. 3 to FM mode, 0 - 5 Hz	(2b) Installed wide-band hi-gain strain in channel No. 2, FM mode, 0.015 - 5 Hz
RF-NV	02 October 1970	21 February 1971	23 April 1971
KP-NV	30 October 1970	28 February 1971	20 April 1971
QM-NV	01 October 1970	13 February 1971	28 April 1971
T1-NV	04 October 1970	06 February 1971	23 April 1971
YM-NV	04 October 1970	25 February 1971	21 April 1971
OB-NV	06 October 1970	11 February 1971	24 April 1971

d. Direct record electronics in the wide-band low-gain strain channel were replaced in February 1971 by FM record electronics to extend the 0.1 Hz low cutoff to dc. (See item 3c in Table 2.)

e. A wide-band high-gain strain channel (0.015 to 5 Hz) was installed in channel No. 2 of the magnetic tape recorder at each of the six sites during the interval 19 to 27 April 1971. (See item 2b of table 2.) The purpose of this channel is to furnish data on the dynamic phase of the strain signal and to serve as a flag for low-level events. This channel accomodates only low-level signals at high frequencies; therefore, the low-gain wide-band channel was retained to preserve large signals.

A schematic of the modified strain channel configuration is shown as figure 2. Frequency response curves are shown in figure 3.

The response of the system to a typical event and to a step calibration is shown in figure 4.

1.3 MAINTENANCE

When operation was resumed in September 1970 the signal control center, recorders, and generators were installed and signals from all sensors were regained with only minor adjustments in range settings and without entering the sealed tunnels containing the strain transducers. Continuity of recording was satisfactorily maintained by the use of spring-wound Esterline-Angus paper recordings. However, loss in continuity of strain signal on the magnetic tape recorders was caused by occasional occurrences of low power output from the thermoelectric generators, in addition to a problem of broken drive belts and drive-motor failures in the tape recorders. Power problems were eliminated in May 1971 when new thermopiles were installed at sites KP-NV and YM-NV. Tape recorders malfunctions were eliminated by the installation of motor replacement kits about 1 June 1971.

Five percent of the strain data was lost when unpredictable short-term temperature changes during intervals of unattended operation caused the output to exceed the range of the system. Most of the loss occurred at site KP-NV.

One month of data was lost at KP-NV between 15 May and 15 June 1971 as a result of accumulation of water in the mine tunnel. The restoration process included pumping residual water from the mine tunnel and replacing the transducer electronics.

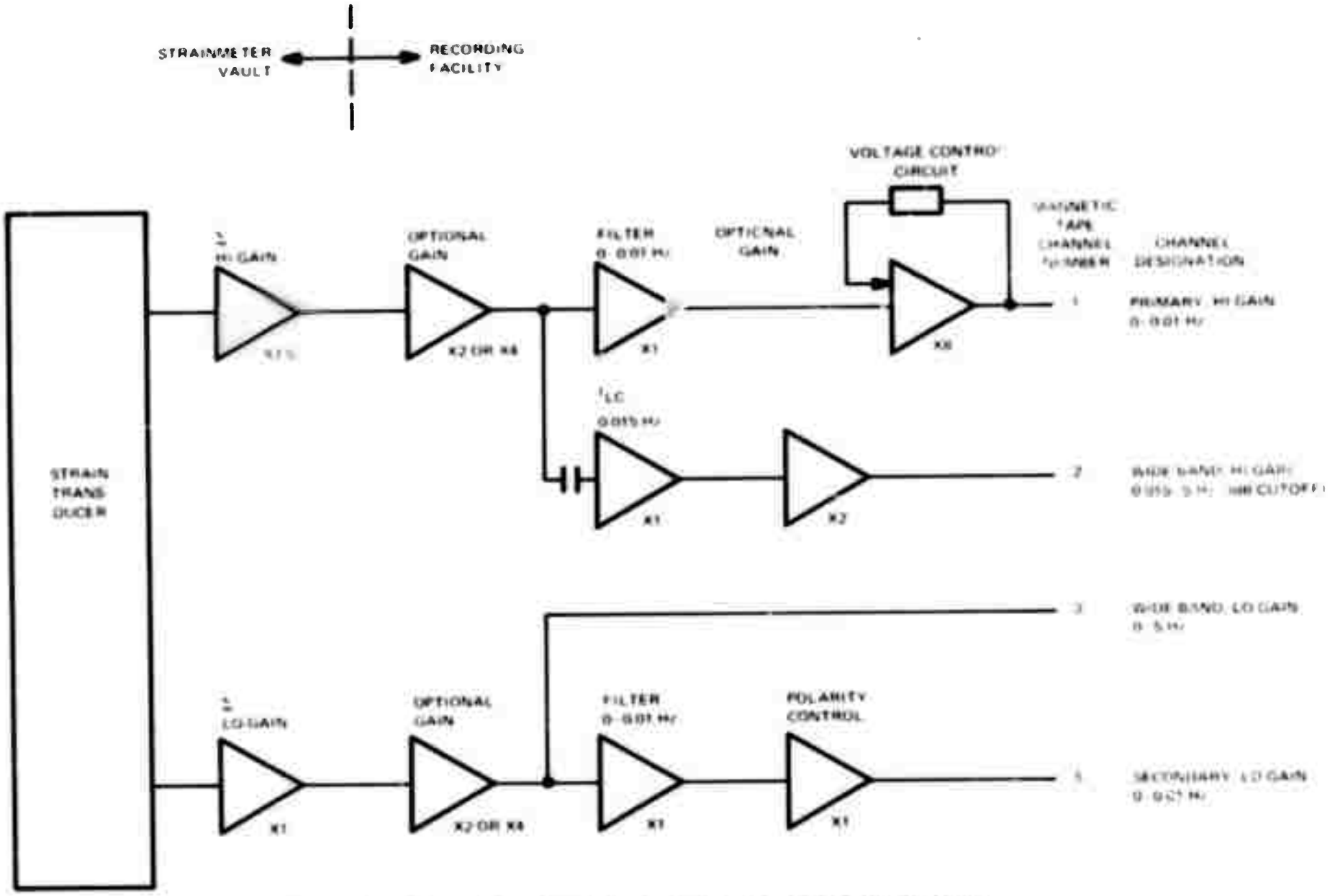

Figure 2. Schematic of modified strain channel configuration

G 6543

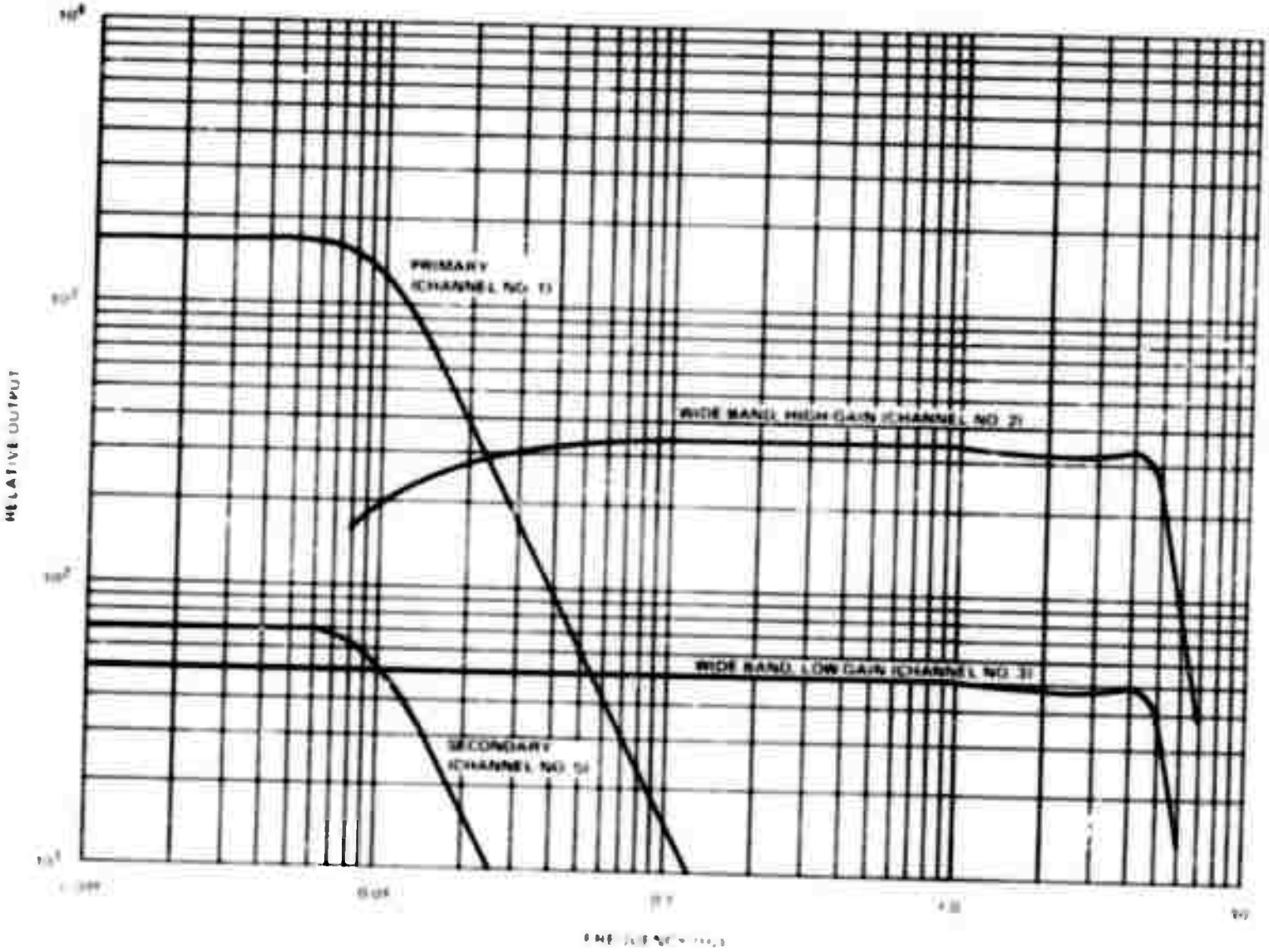

Figure 3. Amplitude response of the modified strain channel configuration in response to differential pier motion

G 6544

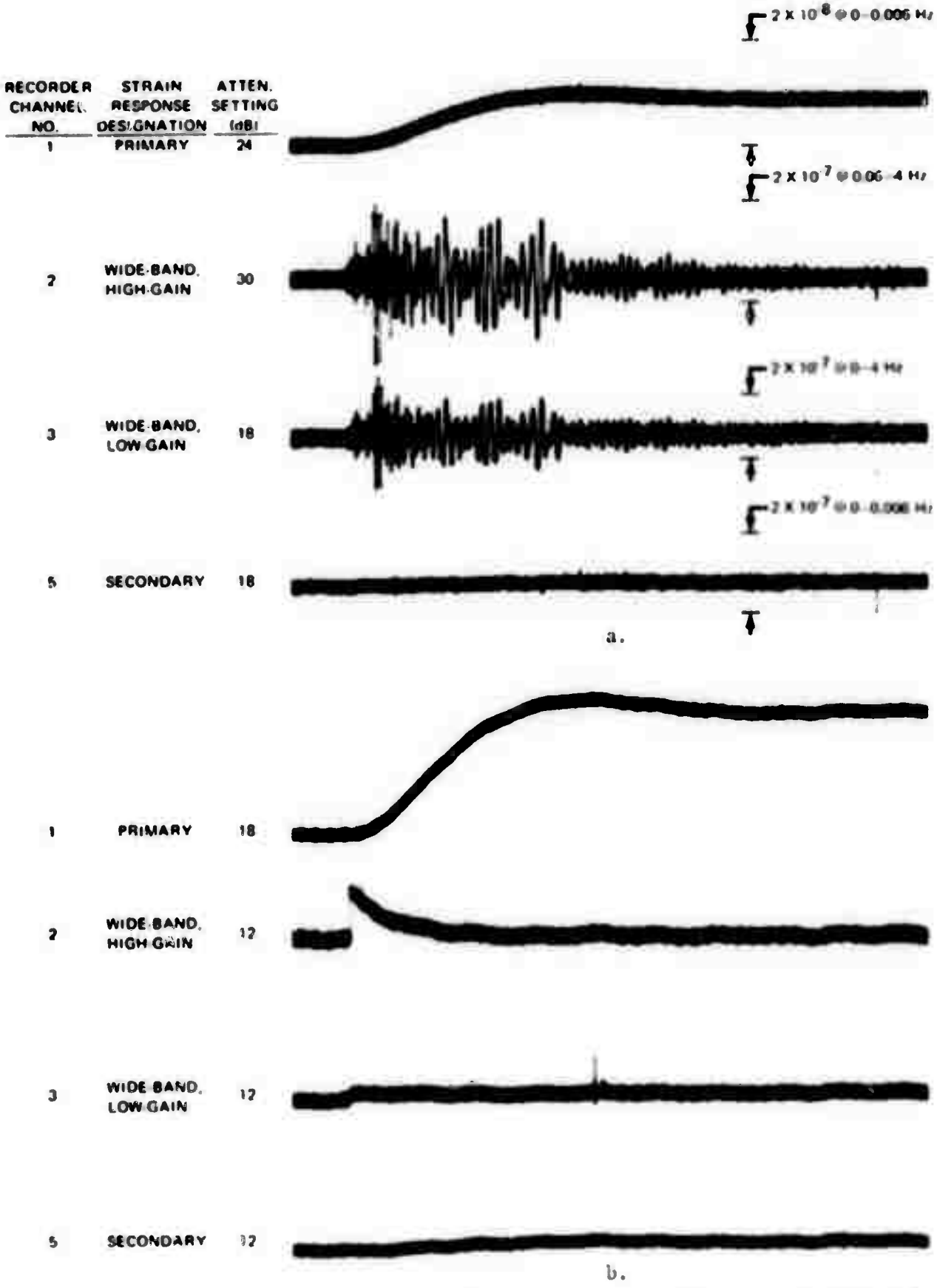

Figure 4. a. Response of the strain channels to a typical NTS event (MINATA, 08 July 1971) recorded at site QM-NV. b. Response to a step function applied with the EM calibrator

2. SECULAR STRAIN

Secular strain measurements from all sites have been plotted in figure 5 for data through July 1971 when operation of the six portable strain sites was terminated. Secular strains as defined here include all strains outside the pass band of seismic signals and diurnal astronomical tides. Observations of secular strain were taken on an average of about once per week for each site. These observations reflect all sources of strain including astronomical tides, diurnal temperature changes, atmospheric pressure changes, seasonal temperature changes, and regional strains. However, tides, diurnal temperature, and pressure influences are negligible when compared to the magnitude of the long-term effects. The maximum change in strain over an 11-month period is listed in table 3 for each site.

Table 3. Secular strains

Site	Maximum seasonal change in strain ($X10^6$ m/m)	Maximum seasonal change in tube temperature (°C)	Seasonal strain coefficient (m/m/°C)	Resultant 1-year change in strain ($X10^6$)
RH-NV	15.6	4.1	3.8	•10.6(c)
KP-NV	17.4	•	•	-10.4(e)
QH-NV	5.3	•	•	• 2.3(c)
TI-NV	14.0	•	•	• 0.2(c)
YM-NV	8.9	5.7	1.6	• 0 (c)
OB-NV	10.2	0.5	20	•8.5 (c)

•Not computed

(c) compression
(e) extension

The relative seasonal changes in strain among the sites are not explainable on the basis of type of installation (trench or tunnel); however, the deeper of the two trench sites (YM-NV) has less seasonal change than the shallower one (TI-NV), and the deeper tunnel (OB-NV) has less seasonal change in strain than either RH-NV or KP-NV. The seasonal change does not appear to be related to the temperature change in the tunnel, as measured on the tube. For example, the ratio of seasonal strain to tube temperature varies from 1.4 x 10^{-6}/°C at YM-NV to 20 x 10^{-6}/°C at OB-NV. The large differences in the ratio are not explained by differences in site coupling coefficients, and are not reasonably related to possible differences in expansion coefficients of the rock among the sites. It is possible, however, that the temperature of the tube does not accurately reflect the temperature of the rock at those depths that most strongly influence strains measured in the tunnels. A typical relationship among strain, tube temperature, and free air temperature over the 11 month operational period is shown in figure 6 for site RH-NV.

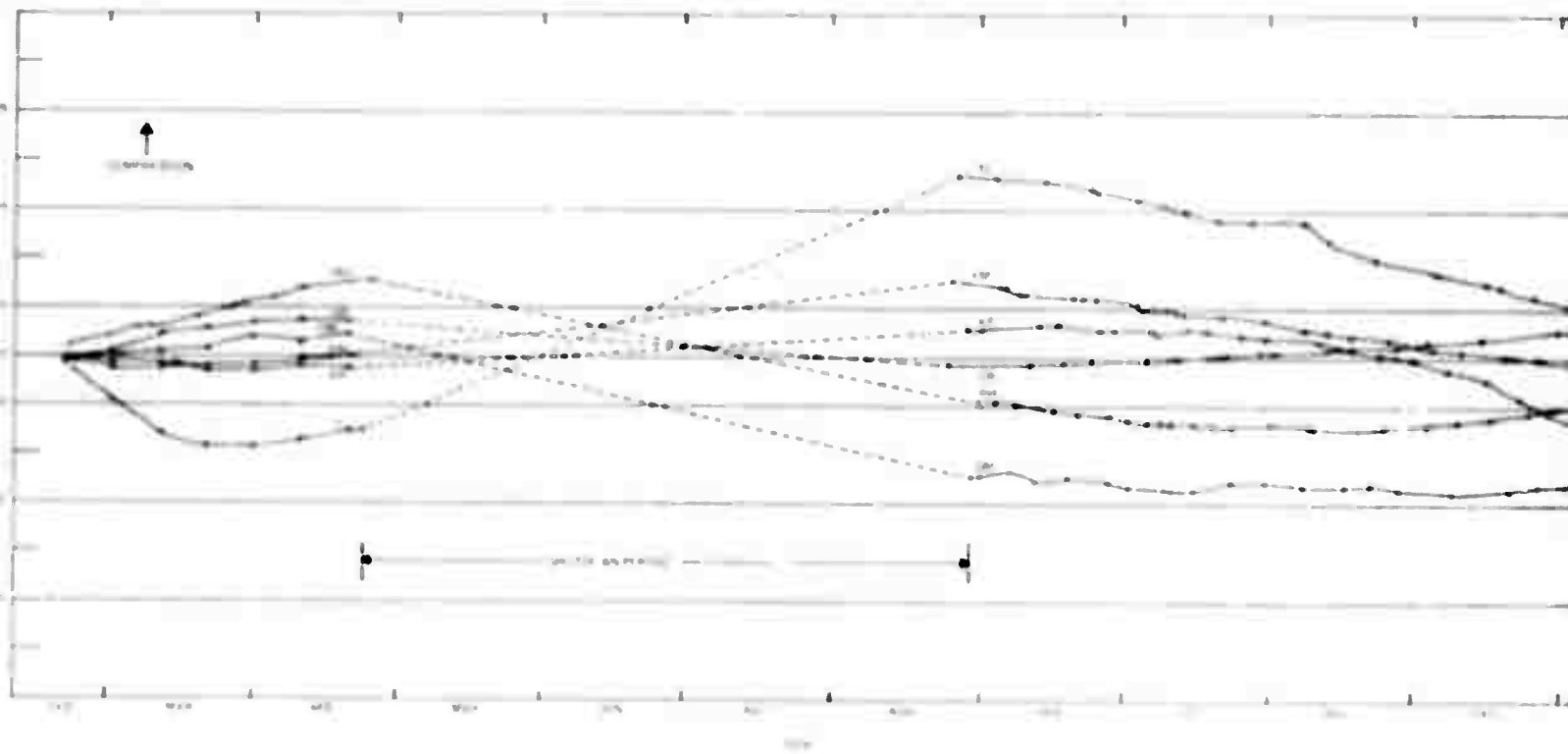

A

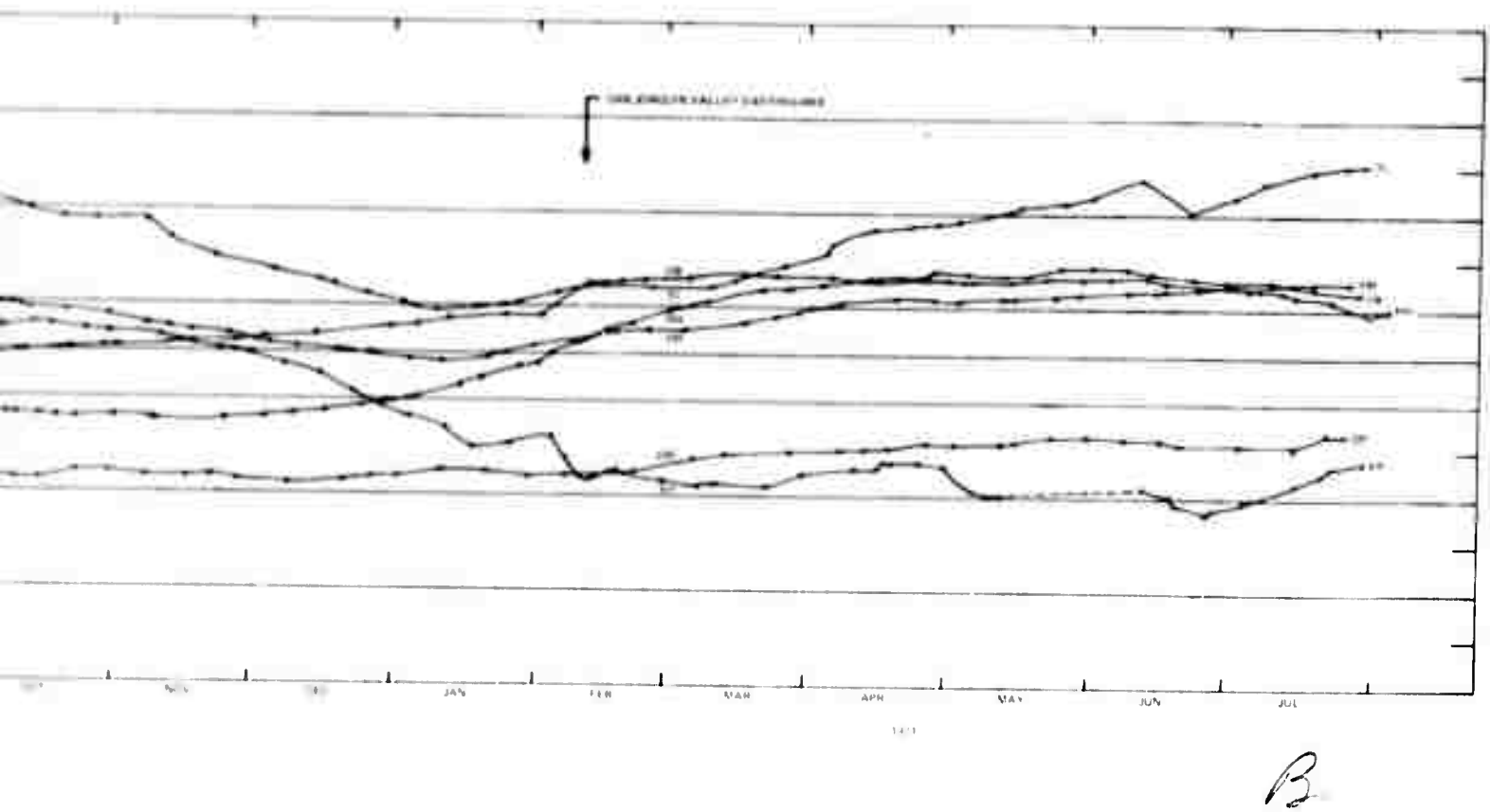

B

Figure 5. Secular strain at six portable strain sites in southern Nevada during the period March 1970 through July 1971.

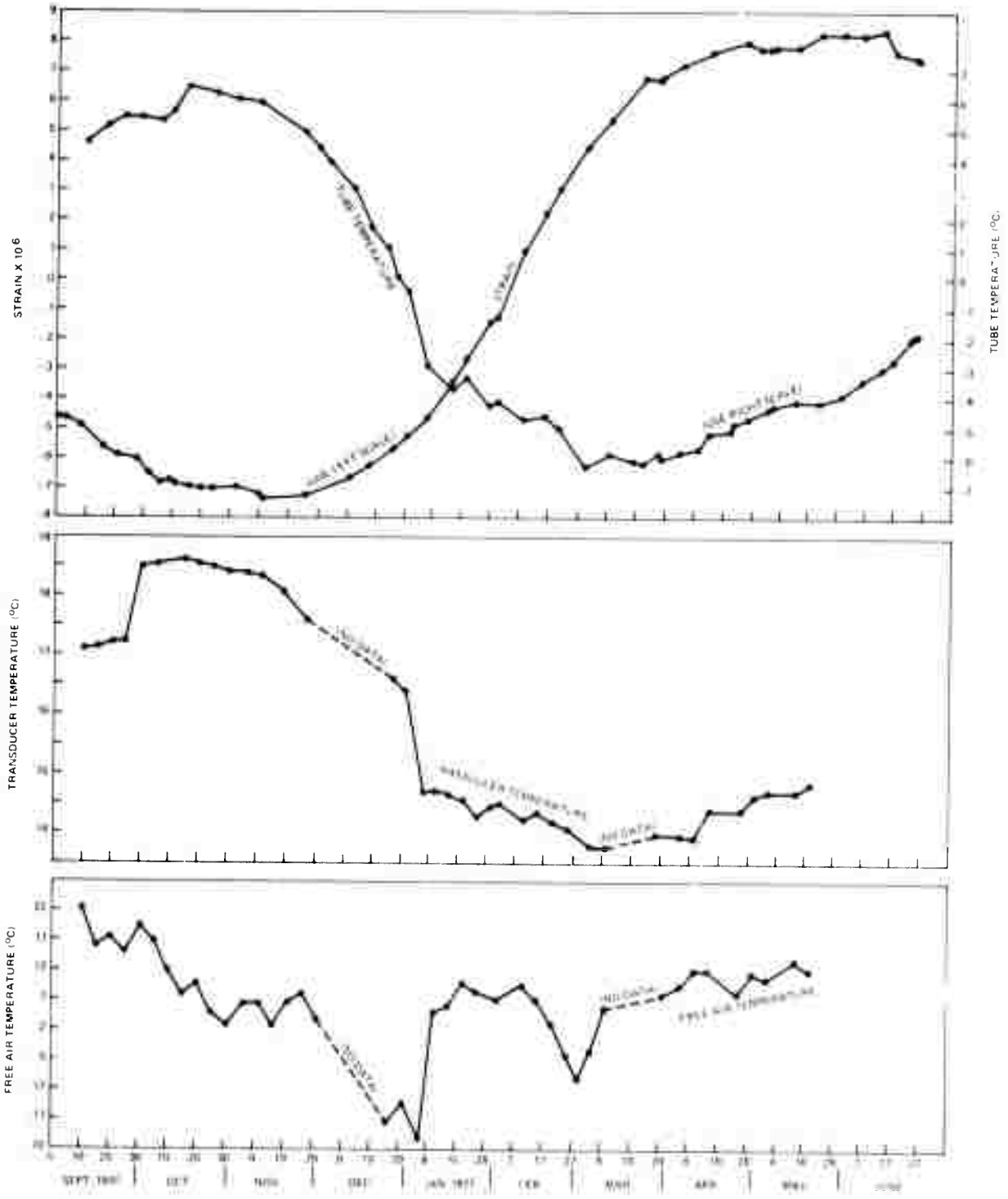

Figure 6. Secular strain and temperature observations at Site RH-NV in the period September 1970 through July 1971

G 6545

Also listed in table 3 is the resultant annual change in strain for each site. It is noted that the two trench sites (TI-NV and YM-NV) show a return to essentially the same strain measured a year earlier. On the other hand, the four tunnel sites show a mean resultant change in strain of 8.3 x 10^{-6} m/m for the 1-year period, which is 68% of the mean of the maximum seasonal strains. Since tunnel temperatures have returned approximately to their original value in the annual cycle, temperature effects have been ruled out as a cause of the substantial 1-year change in strain at several of the sites. Furthermore, the data does not fit any pattern that would suggest a long-term trend in the regional strain field in southern Nevada. Therefore, it is concluded that the resultant change in strain is a condition peculiar to each site, or, at most, to subregions of the area covered by the six sites.

3. COUPLING OF THE TIDES AND EARTHQUAKES

In any study involving earth motion at two or more sites, the degree of coupling of the instruments to the earth or of the surface material to the rock at depth is of primary interest. In the present investigation, coupling factors for each site are needed specifically to determine the correct proportion of theoretical tidal strain to subtract from observed strain in the process of determining the relationship between strain and environmental factors. Initial attempts to subtract the full theoretical tide from the observed strain led to difficulty in interpreting results. Several sources of error were investigated. Large errors in calibration were ruled out, since two independent methods of calibration are used. The accuracy of the tidal data from the program 'ERTITD,' kindly furnished by Dr. Stewart Smith of the University of Washington (the program was originally written by Berger and Farrell at La Jolla and modified by Smith for use on the CDC computer), was compared with a sample of the output of a tidal prediction program furnished by Mr. Gerry Cabaniss, Terrestrial Sciences Laboratory, Air Force Cambridge Research Laboratory. Differences in amplitude approaching 10 percent near the peaks were reported by the Seismic Data Laboratory at Alexandria, where the program was run. The disagreements in the data were considered negligible for the purposes of this study.

Two other factors considered were the possibility that the tidal coupling was frequency dependent and the possibility that tidal data were masked by environmental effects. Smith and Kind (1971) shed light on the latter factor using data from the six portable strain sites from the period December 1970 through January 1971. By comparing absolute values of the Fourier transforms of the observed strain and calculated earth tides, they established that all stations were coupled to the crust, although not to the same extent. They also concluded that most of the stations were affected by thermal and barographic effects based on the fact that most sites showed a larger ratio of 12-hour to 12.42-hour energy.

Using the criteria set forth by Smith and Kind, a similar study of tidal coupling was carried out for the purpose of comparing the results with the coupling of earthquakes. A typical plot of absolute values of the Fourier transform of observed strain and calculated earth tides for site RH-NV are shown in figure 7. Coherence and phase, obtained from cross-spectra, are also shown. The calculations are based on observations at 1-hour intervals over a 30-day period, starting in October 1970. Selected portions of the spectrum have been replotted on a linear scale for all sites (figure 8). The resolution of tidal peaks for sites KP-NV and T1-NV is poor because of the small number of data samples. The ratio of observed strain to calculated earth tides, denoted as apparent tidal coupling factor is listed in column C of table 4 at tidal periods of 12.0, 12.42, 24.0, and 25.8 hours, corresponding to tidal designators S_2, M_2, S_1, and O_1. It is noted that the 12.0-, 24.0-, and 25.8-hour tides are for the most part larger than the 12.42-hour tide, a relationship that could exist if the data were contaminated by thermal and pressure variations. Coherence values for the latter three tidal periods are in general lower than for the 12.42-hour tidal period, suggesting a multi-source generation of energy at those periods.

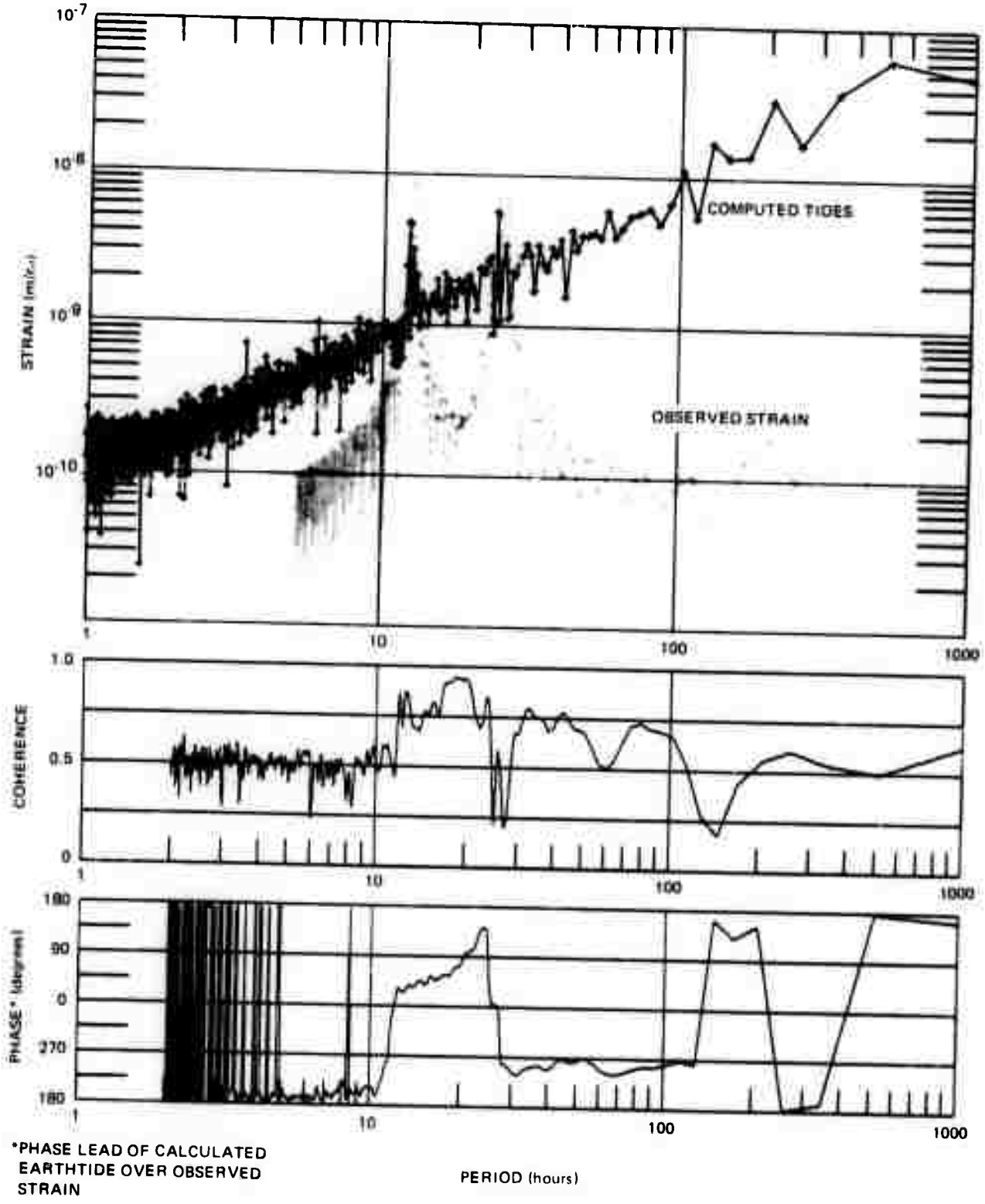

Figure 7. Absolute values of the Fourier transform of observed strain and calculated earth tides along with coherence and phase for site RH-NV from hand-digitized readings at 1-hour intervals over a 30-day period starting on 12 October 1970. 720 samples, 511 lags, Parzen smoothing; 1 sample/hour.

G 6565

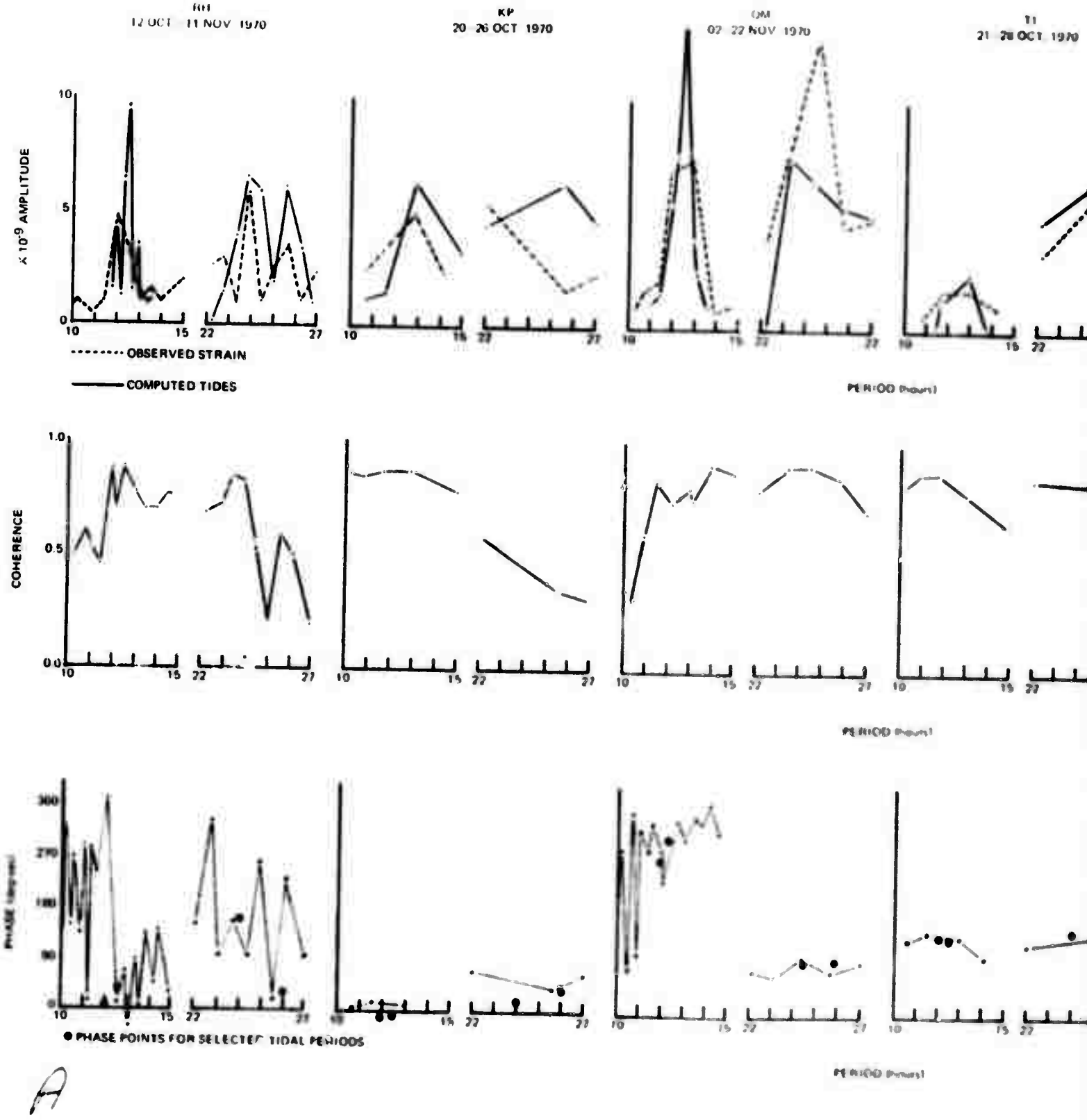
RH
12 OCT 11 NOV 1970
KP
20 26 OCT 1970
OM
02 22 NOV 1970
TI
21 28 OCT 1970
$\times 10^{-9}$ AMPLITUDE
OBSERVED STRAIN
COMPUTED TIDES
PERIOD (hours)
COHERENCE
PERIOD (hours)
PHASE (degrees)
PHASE POINTS FOR SELECTED TIDAL PERIODS
PERIOD (hours)

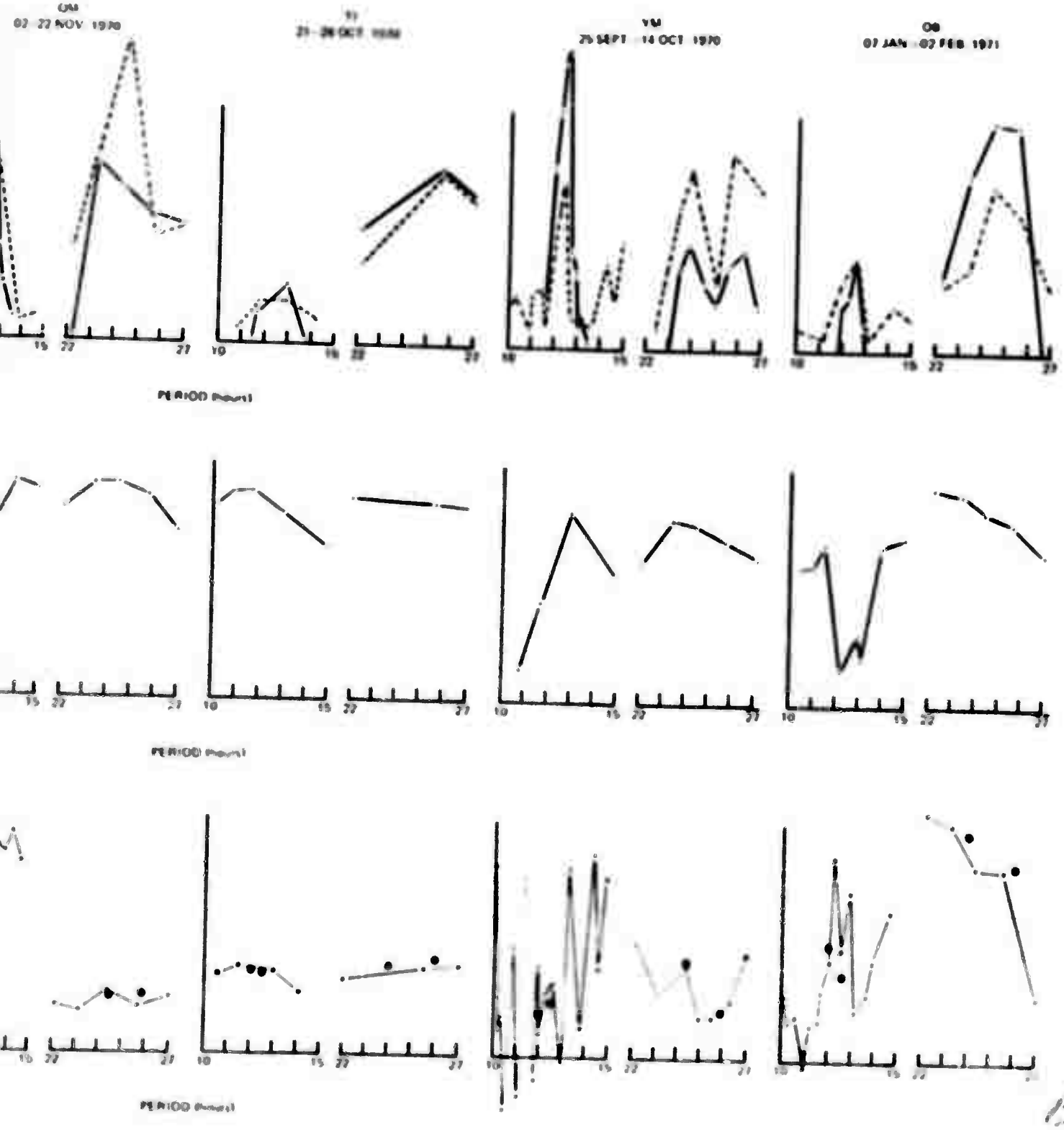

Figure 8. Absolute values of the Fourier transform of observed strain and calculated earth tides along with coherence and phase for selected portions of the spectrum. One sample per hour, 50% lags, Parzen smoothing. Phase is in terms of phase lead of calculated tides over observed strain.

G 6566

Table 4. Apparent site coupling factors (column C) computed from the ratio of observed strain (column B) to the calculated earth tide (column A) for the S_2, M_2, S_1 and O_1 components of the earth tide corresponding to tidal periods of 12.0, 12.42, 24.0, and 25.8 hours, respectively

Site	A Calculated Earth tide ($\times 10^{-9}$)				B Observed Strain ($\times 10^{-9}$)				C Apparent Coupling Factor, B/A			
	S_2	M_2	S_1	O_1	S_2	M_2	S_1	O_1	S_2	M_2	S_1	O_1
RH-NV	12	21	15	12	5.1	3.0	4.5	2.5	0.43	0.14	0.30	0.21
KP-NV	5.9	11	14	12	9.4	9.8	8.1	3.0	1.6	0.90	0.58	0.25
QH-NV	11	26	18	13	17	11	28	13	1.5	0.42	1.6	1.0
TI-NV	3.4	4.5	16	15	5.5	5.1	15	14	1.6	1.1	.94	.93
YM-NV	21	28	8.3	8.3	4.8	13	16	17	.23	.47	1.9	2.0
OB-NV	5.0	9.0	27	20	5.4	11	18	10	1.1	.12	.67	.50

To resolve the question as to whether differences in coupling of the M_2 tide among sites is a tidal related problem or a general site coupling phenomenon that is independent of wave type, we turn to the question of earthquake coupling, a study of which requires the recording of one or more distant earthquakes of Richter magnitude 7 or greater. The system is severely limited in the detection of distant events because it was designed to study the quasi-static and permanent strain changes resulting from explosions of the order of magnitude 6 at distances of approximately 30 to 100 kilometers. A filter with a high cutoff frequency of 0.01 Hz, designed to attenuate high frequency signals from large explosions, unfortunately attenuates waves from large distant earthquakes. However, a fairly useful measure of relative coupling among the six sites was obtained from the measurement of Rayleigh waves from three earthquakes. Rayleigh wave amplitude was corrected for strain azimuthal response ($\cos^2 \alpha$) where α is the angle between the long axis of the strainmeter tube and the direction of wave propagation. Care was taken to select Rayleigh waves from the initial group of a given wave period since the initial group usually arrives at the true azimuth or at slight azimuthal deviations from this, as pointed out by Capon (1970). The selection of wave periods involved a compromise among three requirements: (1) use of the earliest arrivals of a given wave period, (2) maximum signal-to-noise ratio, and (3) absence of Love waves. However, the results indicate that one or more of the foregoing factors contaminated the data. The results of the investigation are listed in table 5 for each of the earthquakes. Coupling factors are normalized to site RI-NV since it is the only site that does not contain a critical angle ($\alpha = 90°$) for Rayleigh waves from any of the earthquakes. The coupling factors are also normalized to unity for site KP-NV which has the highest relative coupling. It is noted that RI-NV and OB-NV have low coupling factors. Data for Rayleigh waves arriving at an extremely critical azimuthal angle were omitted from table 5. A case in point is the coupling factor for YM-NV for the event from New Ireland on 14 July 1971, which had an azimuthal correction factor of 0.015 (table 6) at an approach angle of 083° (figure 9). If the calculated approach angle (α) were in error by say 2°, e.g., 085° instead of 083°, the corrected amplitude of the Rayleigh wave, and consequently, the coupling factor would have been in error by a factor of two. Contamination by Love waves is also a problem at this angle.

The use of Love wave amplitudes yielded a larger spread of values of relative coupling for a particular site than obtained for Rayleigh waves. Possibly, the greater sensitivity of strainmeters to changes in the azimuth angle of Love waves contributes to the larger spread. The lack of orthogonal horizontal components at a site makes it difficult to resolve the question. Nevertheless, the Love wave signal was very useful in verifying that the instrument polarity at each site was correct.

Tidal coupling and earthquake coupling are compared in figure 10. Four tidal periods (12.0, 12.42, 24.0, and 25.8 hours) from table 4 are compared with the average relative coupling factor for the earthquakes listed in table 5. The occurrence of approximately matched relative coupling ratios among the sites for the M_2 (12.42 hour) component of the earth tide and earthquake surface waves indicates that marked differences in site coupling do exist and tends to disprove the existence of frequency-dependent coupling. The

Table 5. Relative coupling factors computed from Rayleigh waves from three large, distant earthquakes

Site	(1) 10 Jan 1971	(2) 09 July 1971	(3) 14 July 1971	Average coupling factor	Coupling factor normalized to unity at KP-NV
RI	1.0	1.0	1.0	1.0	0.2
KP	-	5.0	-	5.0	1.0
QM	-	5.0	3.0	4.0	0.8
TI	3.0	3.7	2.2	3.0	0.6
YM	-	3.5	-	3.5	0.7
OB	1.3	1.8	0.5	1.2	0.2

(1) Origin West New Guinea, 07:17:03.7Z, 10/01/71, 3.1S 139.7E, M_b = 7.3, M_s = 8.0

(2) Origin Chile, 03:03:18.7Z, 09/07/71, 32.5S 71.2W, M_b = 6.6

(3) Origin New Ireland, 06:11:29.1Z, 14/07/71, 5.5S 153.9E, M_s = 7.9

Table 6. Relative site coupling factors computed from 20-second Rayleigh waves from the New Ireland earthquake of 14 July 1971

Site	Δ (km)	Azimuth station to epicenter (degrees)	Azimuth of strainmeter (degrees)	Approach angle (α) (degrees)	Azimuthal correction factor for Rayleigh
RI-NV	10356.93	265.5	325	60	0.25
KP-NV	10347.25	265.5	356	91	.001
QM-NV	10356.76	265.5	020	65	.18
TI-NV	10305.80	265.2	266	1	1.0
YM-NV	10330.27	265.3	182	83	.015
OB-NV	10377.39	265.7	081	5	.99

Site	Signal amplitude (mm)	Strain sensitivity (1×10^{-9}/mm)	Earth strain	Azimuthal correction factor	Strain corrected for azimuth	Relative coupling factor
RI-NV	6.5	1.18	7.7	0.25	30.7	1.0
KP-NV	13.3	1.05	14.0	0	-	-
QM-NV	11.2	1.45	16.2	0.18	90.	3.0
TI-NV	14.7	4.7	68.5	1.0	68.5	2.2
YM-NV	0	1.39	0	0.015	-	-
OB-NV	11.8	1.16	13.7	0.99	13.8	0.5

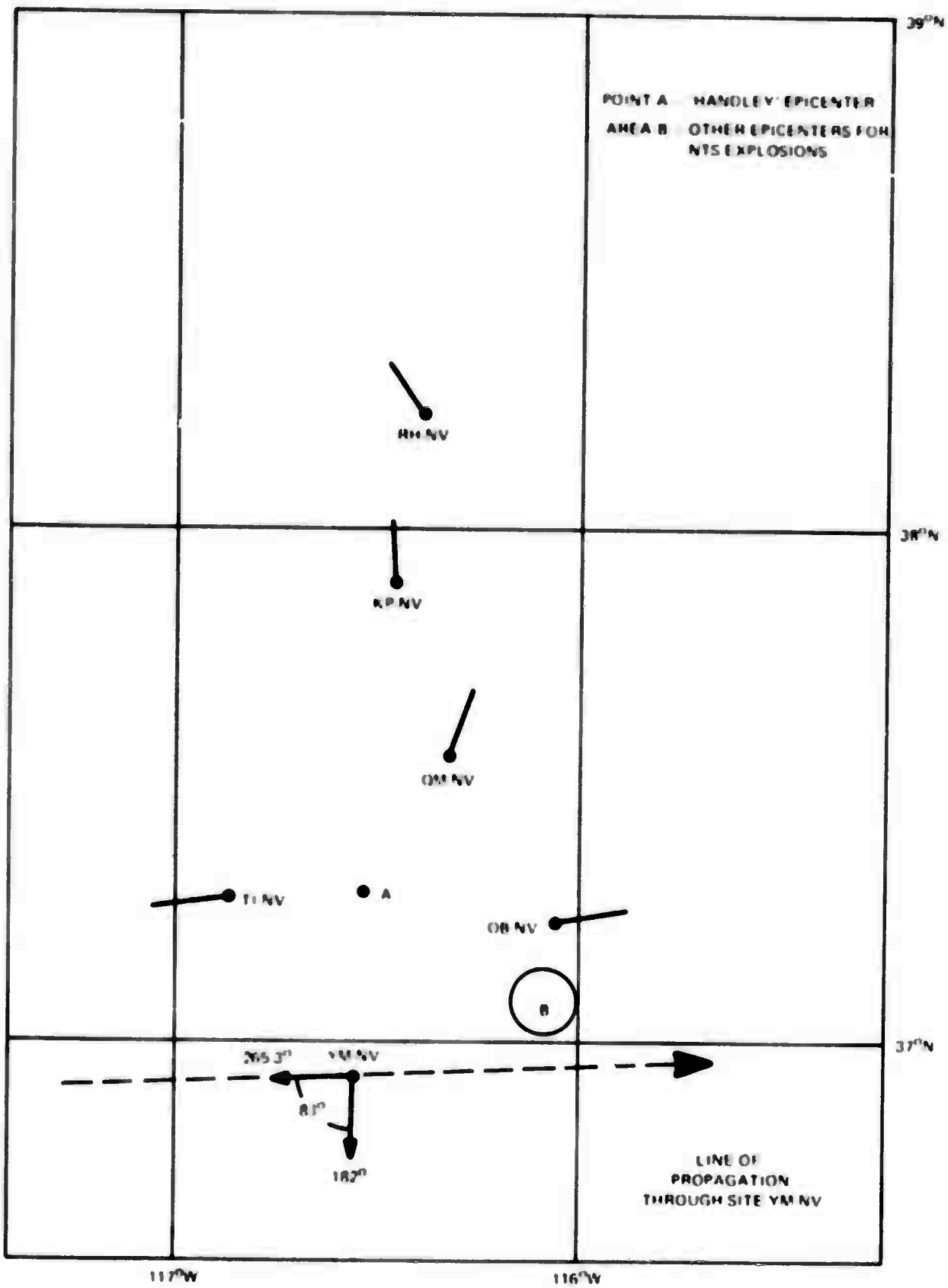

Figure 9. Orientation of the strainmeter at site YM-NV relative to the line of propagation of the New Ireland earthquake of 14 July 1971.

G 6567

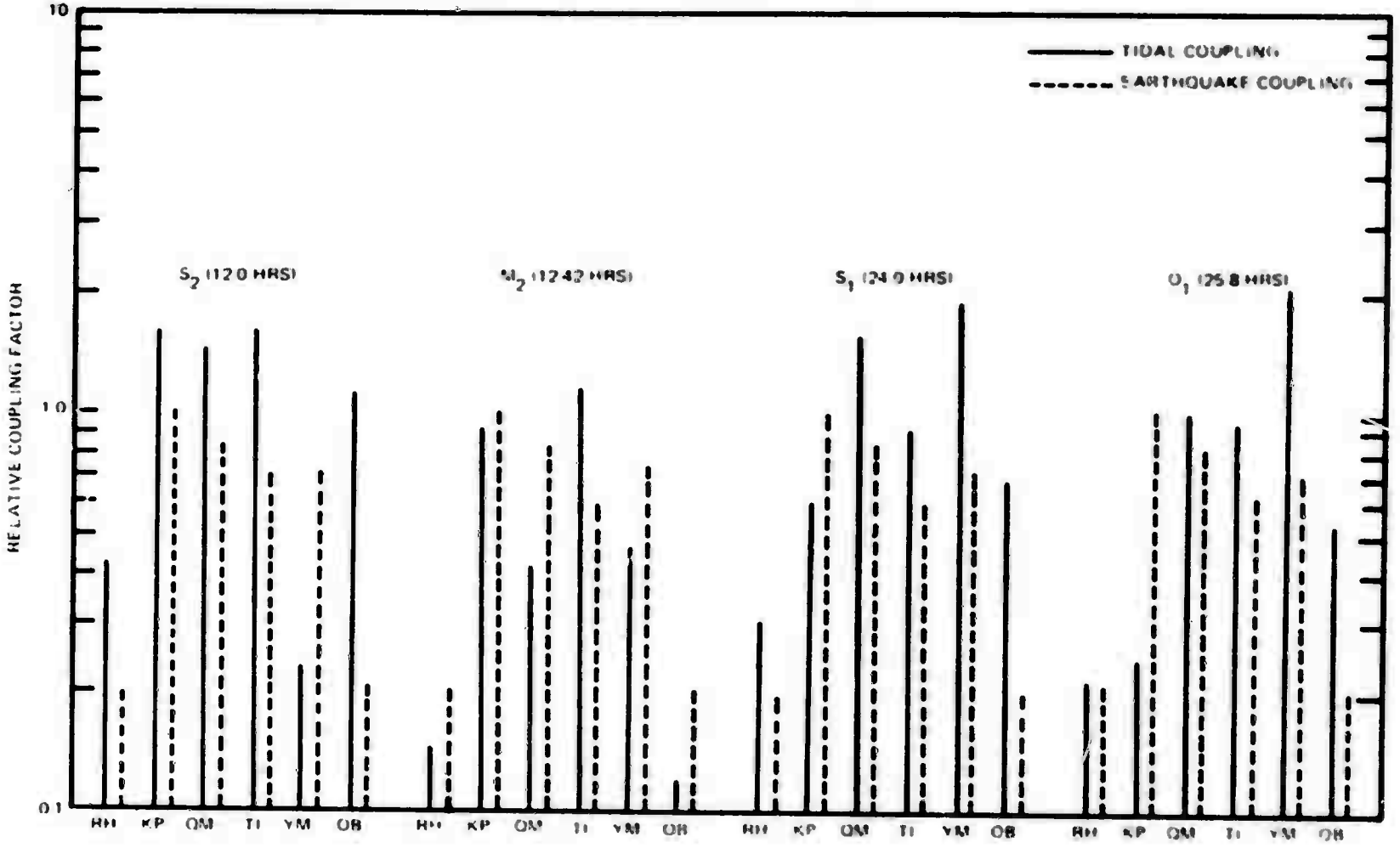

Figure 10. Apparent coupling of the earth tides at periods of 12.0, 12.42, 24.0, and 25.8 hours compared with the average relative coupling factor of earthquake-generated Rayleigh waves in the period range 20-40 seconds.

G 6568

occurrence of abnormally large amplitudes at periods of 12.0, 24.0, and 25.8 hours relative to 12.42 hours, together with a general reduction in coherence indicates the presence of temperature and pressure effects. The presence of these effects to different degrees at different sites is indicated by a wider range of differences between tidal coupling and earthquake coupling at 12.0, 24.0, and 25.8 hours compared with the 12.42-hour tide.

Looking at the M_2 tidal component in figure 10, we note that the coupling factor for sites RH-NV and OB-NV are of the order of a factor of three less than the other four sites. Mechanical hysteresis in the strainmeter can be discounted as a source of low coupling based on tests involving manually-induced forces on the tube anchor, electromagnetic forces between anchor and tube, motor-driven displacements in the transducer, and explosion-induced forces between the earth and the strainmeter, using small dynamite charges at close range.

The relationship between geological characteristics and coupling factors was also investigated. Listed in table 7 are site features that might have some bearing on site coupling. Information on rock type, topography, and faulting are based on USGS Quadrangle Sheets, whereas, estimated values of relative rock competency among the sites are based on on-site observations. Estimates of competency of the rock as related to strain coupling are neither quantitative nor exact. The procedure for estimating competency is based on a qualitative evaluation of the following:

a. The density and hardness of the rock;

b. The degree of fracturing and jointing;

c. The reaction of the rock to the drilling of anchor holes for the strainmeter;

d. The degree of faulting in the vicinity of the site.

Looking for features common to RH-NV and OB-NV that would explain the occurrence of low coupling, we note from table 7 that neither the type of rock nor the estimated competency appear to bear a logical relationship to the degree of signal coupling. In fact, contrary to expected, site QM-NV is well coupled despite the fact that the strainmeter is poorly anchored in strongly altered and highly fractured rock in an area of severe local faulting. If any of the site features in table 7 bear a relationship to site coupling, it is topography, where it is noted that both RH-NV and OB-NV are tunneled into sharp ridges - RH-NV at about 30° to the ridge line, and OB-NV normal to the ridge line. The other four sites lie on the sides of either valleys, low hills, or gently sloping terrain.

Table 7. Summary of geological features of the portable strain sites

Site	Earthquake coupling factor	GEOLOGICAL FEATURES: Estimated rock competency(1)	Rock type	Major faulting	Local minor faulting	Topography
RH-NV	0.2	5	Sheared altered metasediments	4 km east(2)	-	Sharp ridge (tunnel 30° to ridge line)
KP-NV	1.0	3	Volcanic dacite complex	6 km SW(2)	-	Tunnel in flank of steep valley
QM-NV	0.8	6	Altered volcanic dacite complex	5 km east(2)	Area severely cross-faulted; nearest fault is 50 m south	Tunnel in flank of low hill
TI-NV	0.6	4	Altered bedded tuff; fissures not filled	-	-	Trench on gentle slope
YM-NV	0.7	2	Welded volcanic tuff; homogeneous fine grained; clay-filled fractures	-	Moderate faulting starting 400 m NW of trench	Trench on gentle slope
OB-NV	0.3	1	Dolomitic limestone	1.6 km east(2)	Moderate NNW trending; nearest fault is 200 m NW of of tunnel	Sharp ridge (tunnel 90° to to ridge line)

(1) No. 1 indicates the highest rock competency

(2) North trending major high angle fault

4. REMOVING TIDE AND TEMPERATURE-INDUCED STRAINS

In order to determine the decay character of a strain step, the solid earth tides and the temperature-induced strains must be removed from the recorded data. In studying the relation between strain and temperature, principal attention was given to site RII-NV which contained auxiliary control instrumentation. Data in the period 12 October to 11 November 1970, were selected for study initially because of the low seasonal strain rate during this time. Power spectral density plots from 1440 hand digitized data samples of strain, along with temperatures measured in the free-air, in the signal control center, on the tube of the strainmeter, and on the strain transducer, are shown in figure 11. Semidiurnal and diurnal peaks are common to the five power spectra. Coherence and phase between the strain and the temperature observations are shown in figure 12. The results clearly indicate that a large percentage of the strain is related to temperature measured at the transducer for periods through the diurnal cycle. High coherence between strain and transducer temperature in contrast to low coherence between strain and free-air temperature indicates that strains at site RII-NV in the 30-day time period investigated are more strongly influenced by changes in temperature of the strainmeter rather than by surface strains that are transmitted to depth. This conclusion is borne out by data from the same time period displayed in the time domain. Changes in strain relative to changes in free-air temperature show approximately a 9-hour lag in contrast with essentially a zero lag in relation to changes in temperature of either the transducer or the quartz tube. Looking at the phase order of the temperature curves in figure 12, we note that the free air temperature leads the other temperatures as expected, and that the phase difference becomes small at long time periods as expected. A positive polarity is given to compressional strains and increasing temperatures for the data of figure 12. Erratic phase data for all but the transducer temperature have been deleted from the plot in the period interval 1-10 hours.

The relation between strain and atmospheric pressure at RII-NV was examined using data covering a shorter interval of time (12-24 October 1970). Figure 13 shows power spectral density curves for strain, pressure, and temperature using 293 samples at 1-hour intervals. Coherence and phase between strain and the other parameters were obtained using 128 lags.

Only data points at 12, 24, and over 100 hours corresponding to peaks in the power spectral density plot, are plotted in figure 13. The most reliable and most significant point is at a period of 24 hours where temperature effects will have completed a diurnal cycle and the long term seasonal rate of change of strain can be removed. Here, we observe that the strain is in phase with pressure. The results indicate that most of the noise in this 30-day time period could be eliminated from the strain recordings by using a Wiener optimum filter designed to predict the temperature and pressure-induced noise on the strain record. The possibility exists that multichannel filters using all the thermistor readings to predict the temperature-induced strain noise would be even more effective.

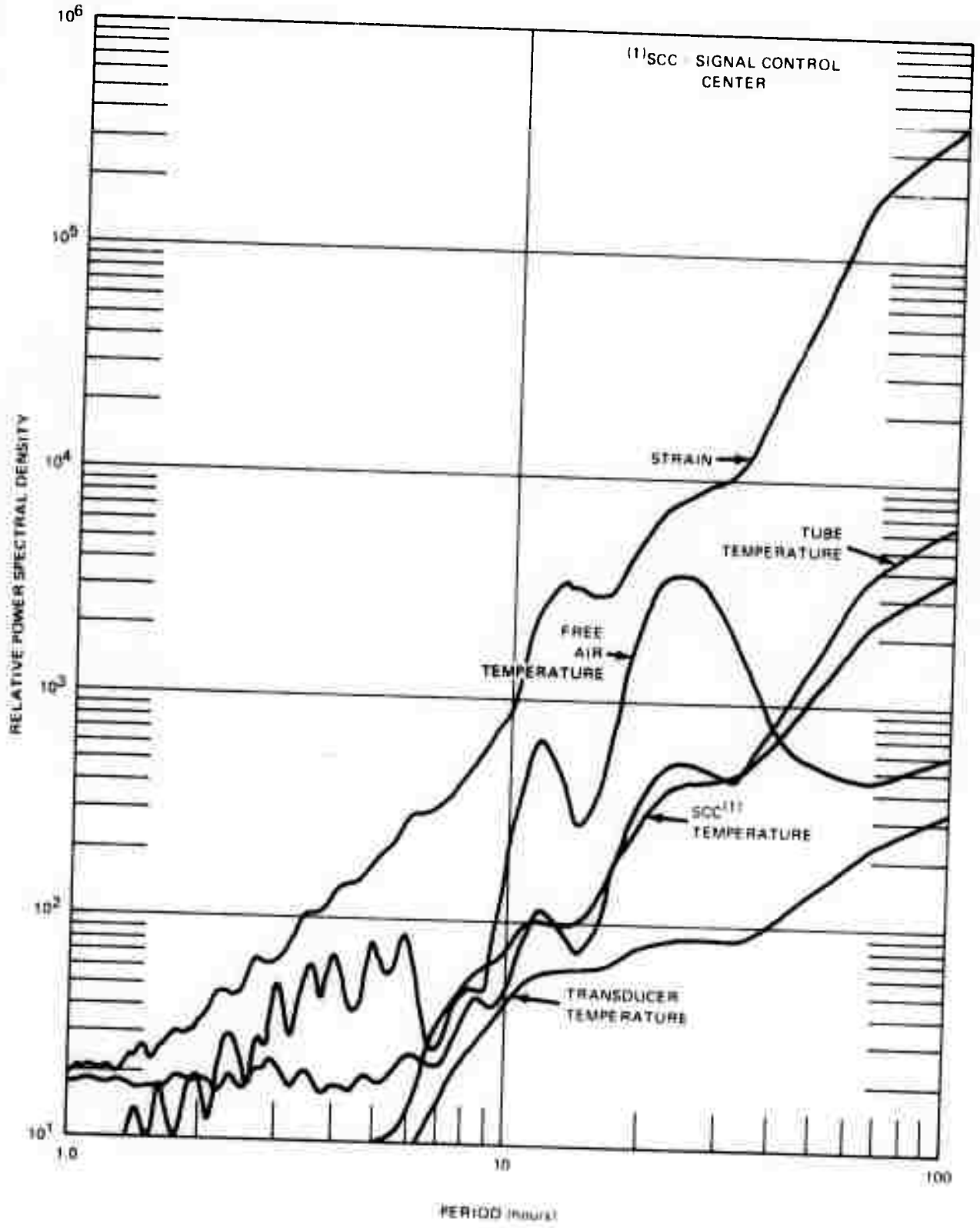

Figure 11. Relative power spectral density of strain, free-air temperature, and instrument temperatures, at site RH-NV from hand-digitized readings at 1/2-hour intervals in the period 12 October to 11 November 1970. 1440 samples, 2 samples/hour, Parzen smoothing.

G 6569

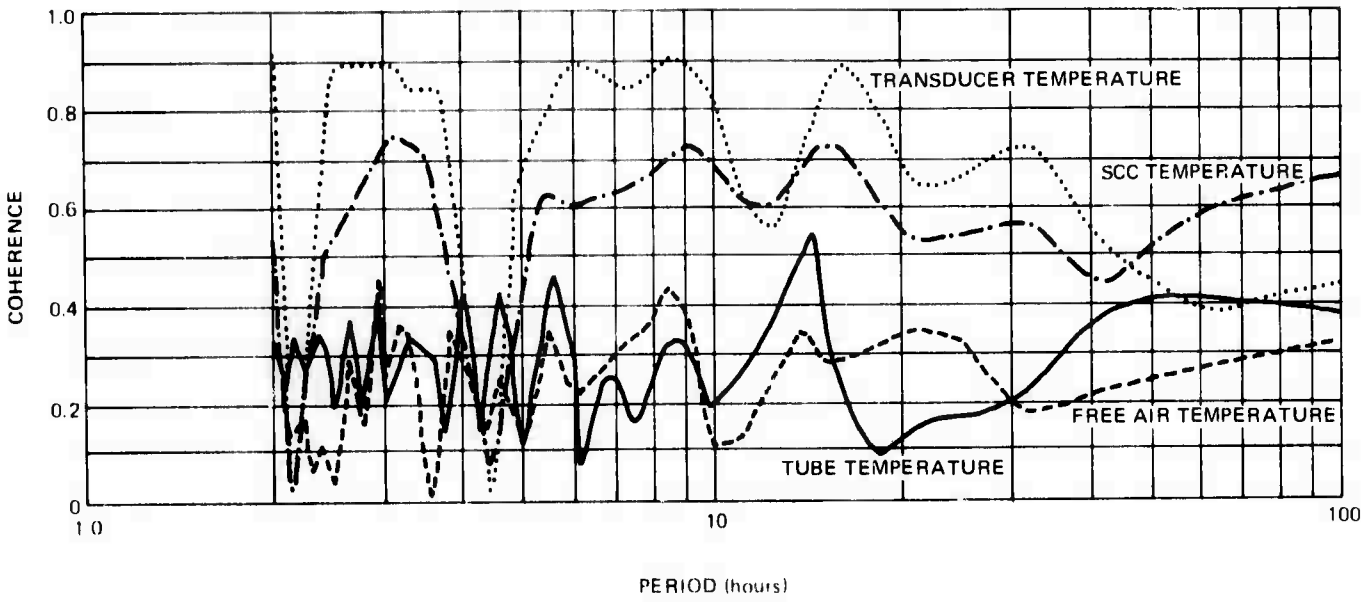

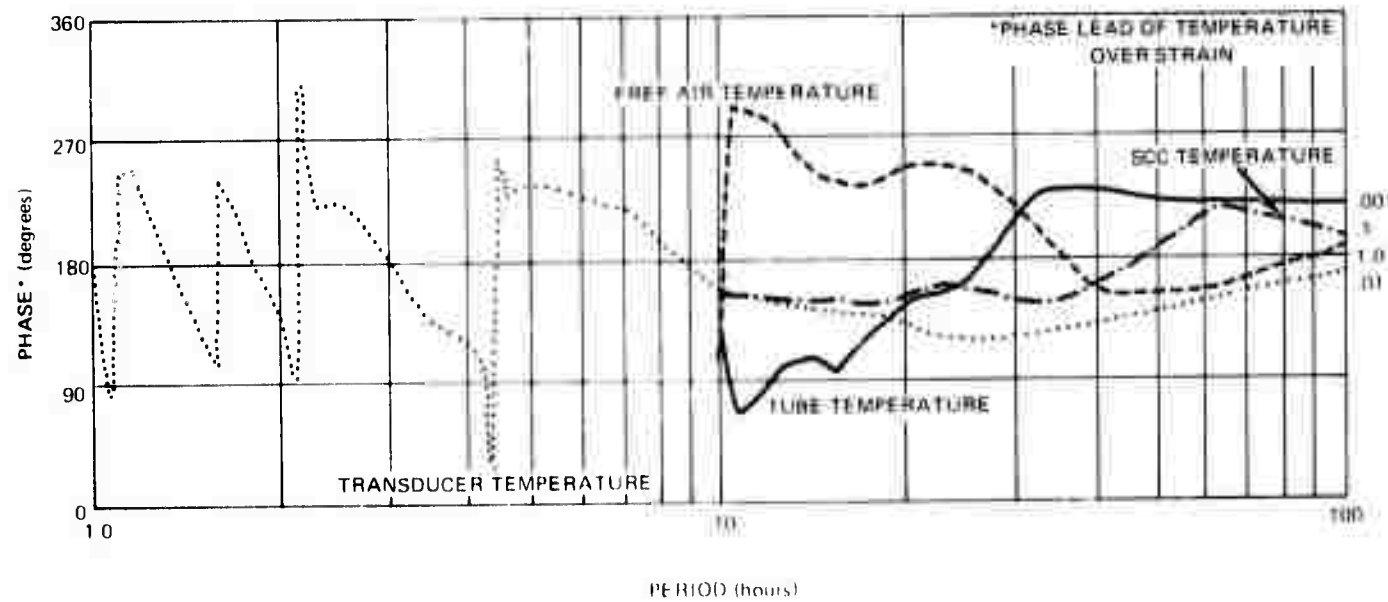

Figure 12. Coherence and phase between strain and temperature measured in the time period 12 October to 11 November 1970 for site RH-NV. 1440 samples, 2 samples/hour, 128 lags, Parzen smoothing.

G 6570

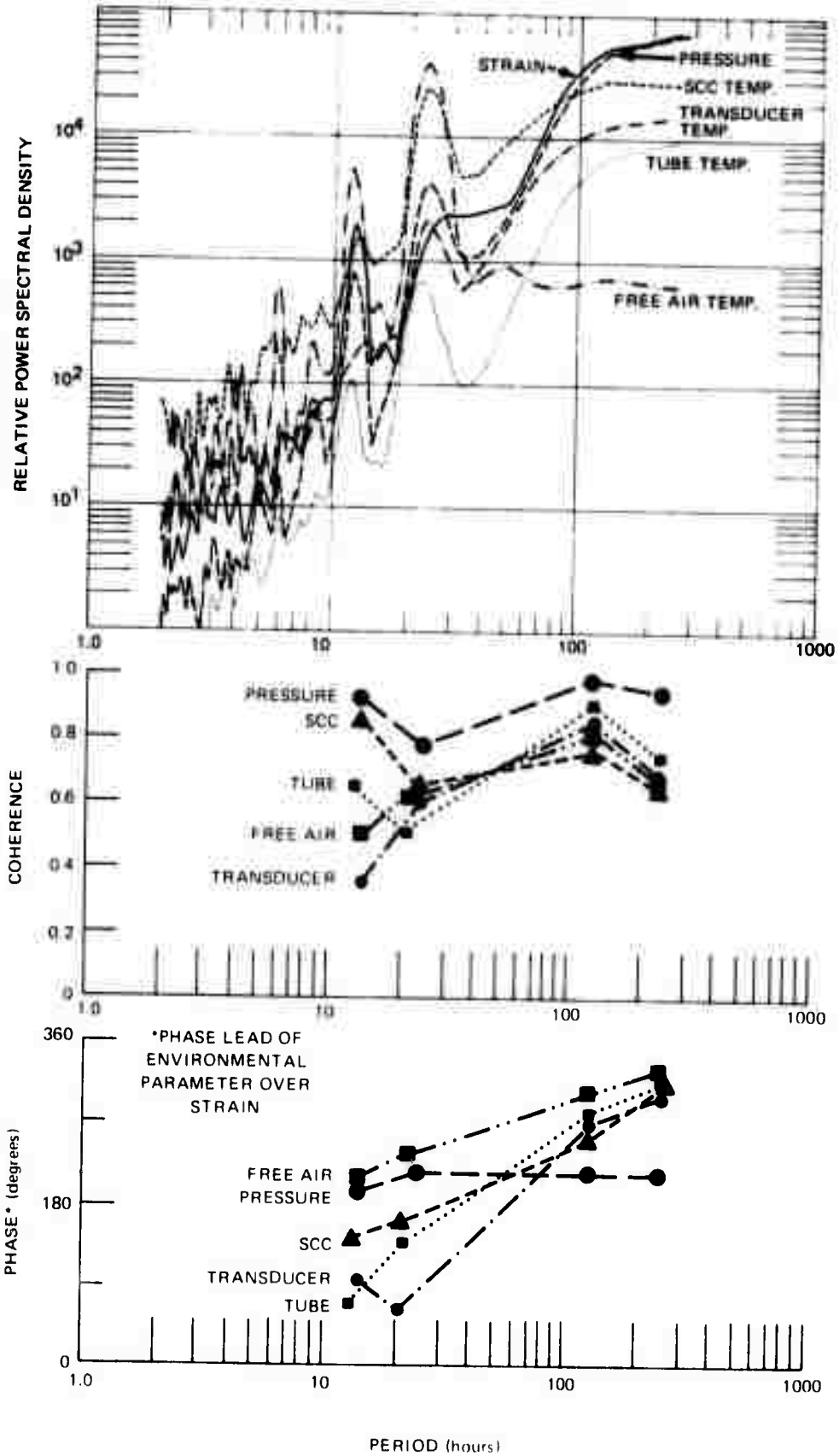

Figure 13. Power spectral density of strain, atmospheric pressure, and various temperatures (upper plot). Coherence and phase between strain and environmental parameters are plotted only for periods corresponding to peaks in the power spectrum. 293 samples, 128 lags, 1 sample/hour, Parzen smoothing.

G 6571

Data from RH-NV in the time interval 08-26 January 1971, during which time a steep rate of strain prevailed, were examined to obtain additional information on the strain-pressure relationship and to determine whether the transducer temperature continues to be a key to eliminating temperature-induced strain from the recording. Simple linear regression analysis was used to determine controlling factors, to systematically isolate both short- and long-term effects, and to derive a relationship between strain and environmental factors. Correlation coefficients were computed for strain as a function of outside air temperature, tube temperature, transducer temperature, and atmospheric pressure. A series of two variable scatter diagrams along with correlation coefficients were obtained for 19 daily observations; 48 hourly observations; and 72 observations at 5-minute intervals.

A correlation coefficient of -0.72 for strain versus tube temperature for the 19 daily observations is interpreted as a compressional strain of the country rock with decreasing seasonal temperature at a rate of approximately $6 \times 10^{-6}/°C$. The temperature effect on the tube, which acts in the opposite direction at a rate of $0.5 \times 10^{-6}/°C$, has not been removed from the observations.

For short-term observations, the strain-temperature coefficient changes sign but retains the same level of correlation. Hourly observations over a 2-day period (17-18 January 1971) show an equivalent extensional strain with decreasing tube temperature at a rate of approximately $0.5 \times 10^{-6}/°C$ as shown in the scatter diagram of figure 14, in close agreement with a predicted strain rate of $0.8 \times 10^{-6}/°C$ for the strainmeter. Tidal strains and a seasonal strain trend of 1.6×10^{-7} per day (figure 15) have been removed. Hourly readings of strain, temperature, and pressure over the 2-day period are shown in figure 16. The high degree of correlation between strain and tube temperature is evident.

The correlation coefficient for strain and atmospheric pressure fluctuations for daily readings, increasing to 0.6 for hourly observations and 0.7 for observations at 5-minute intervals is low (0.12).

At an observation rate of 12 per hour, the strain-temperature rate is approximately $0.4 \times 10^{-6}/°C$ as shown in the scatter-diagram of figure 17 for the time period 1500 to 2040Z on 18 January 1971. Tidal strains and the long-term strain trend have been removed. The data are also shown plotted as function of time in figure 18.

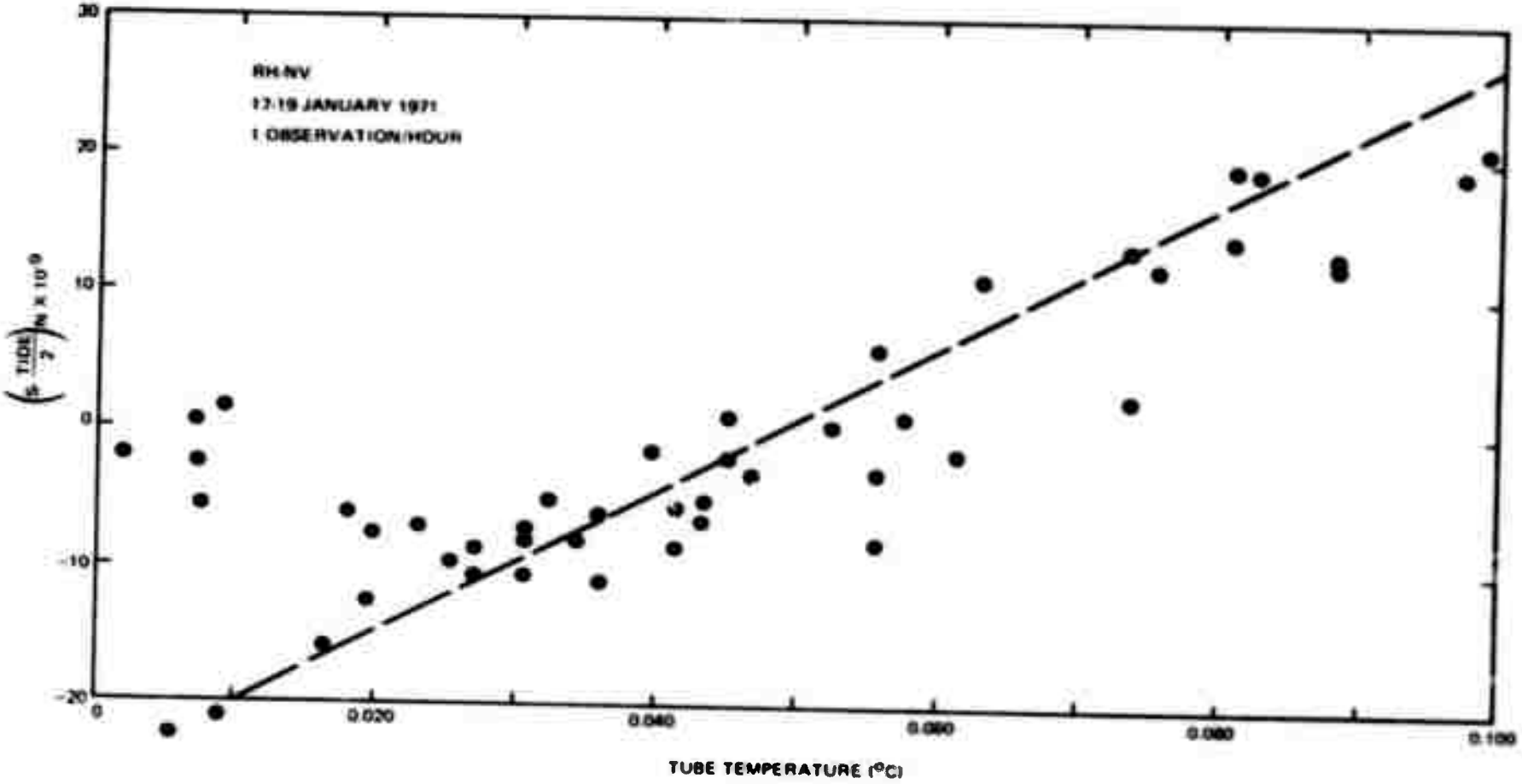

Figure 14. Scatter diagram of hourly observations of strain and tube temperature over a two day time period at site RH-NV. The data, normalized for seasonal trend, show an equivalent strain with decreasing tube temperature at a rate of 0.5 x 10^{-6}/°C.

0 6549

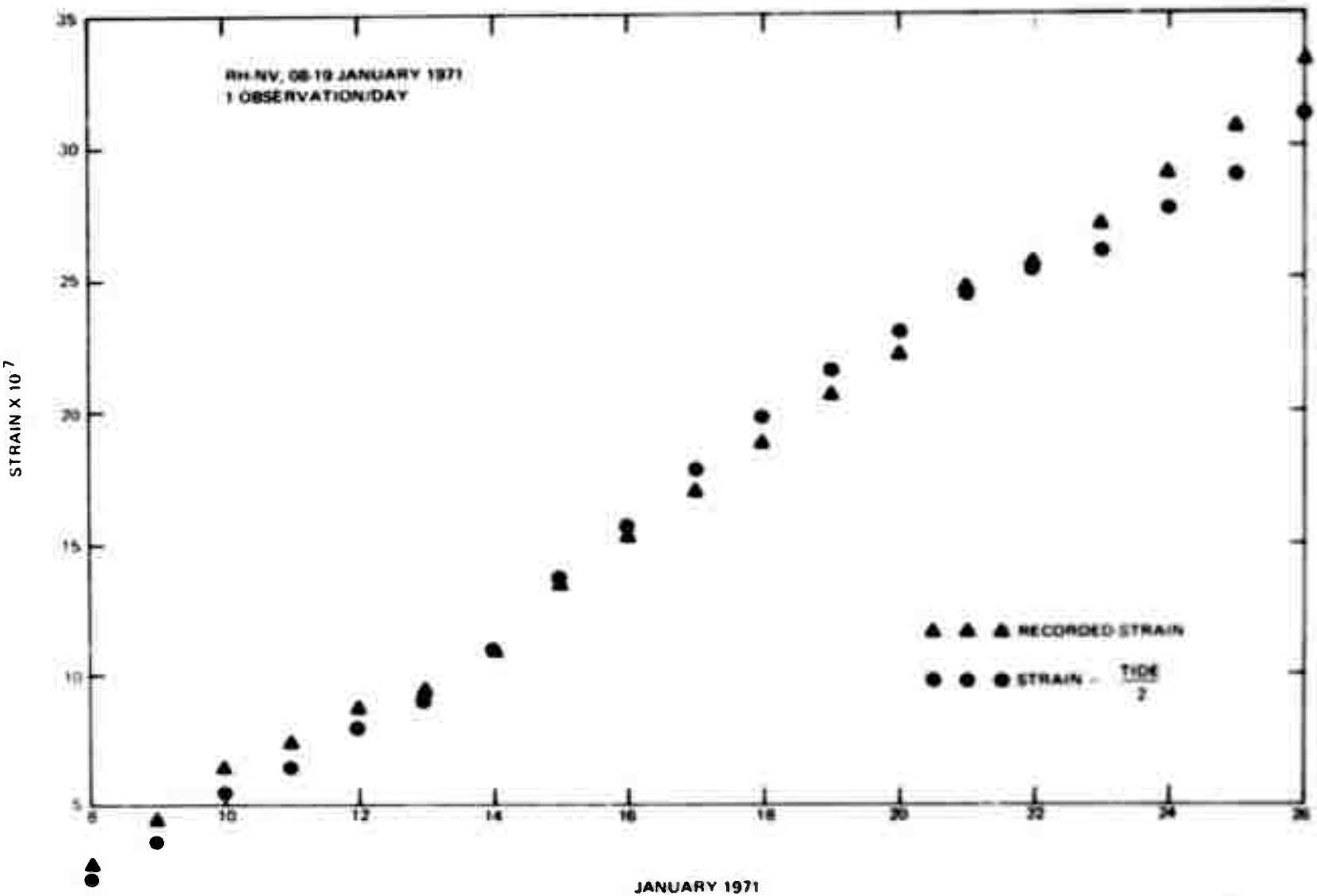

Figure 15. Time plot of daily observations of strain showing a seasonal strain trend of 1.6×10^{-7} per day over an 18-day period (08-19 January 1971) at site RH-NV.

0 6550

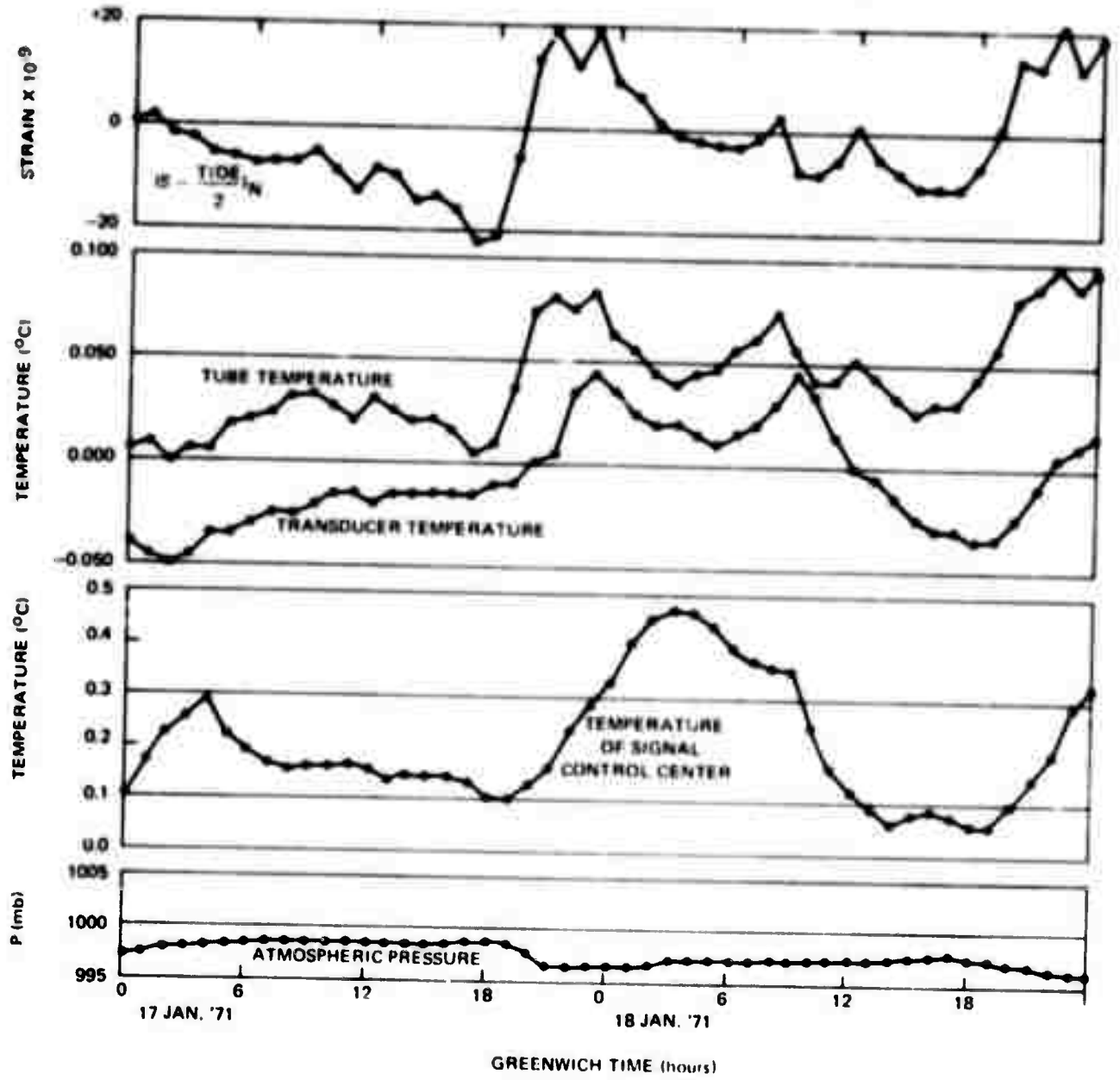

Figure 16. Hourly readings of strain, temperature, and pressure at RH-NV showing high degree of correlation between strain and tube temperature.

G 6551

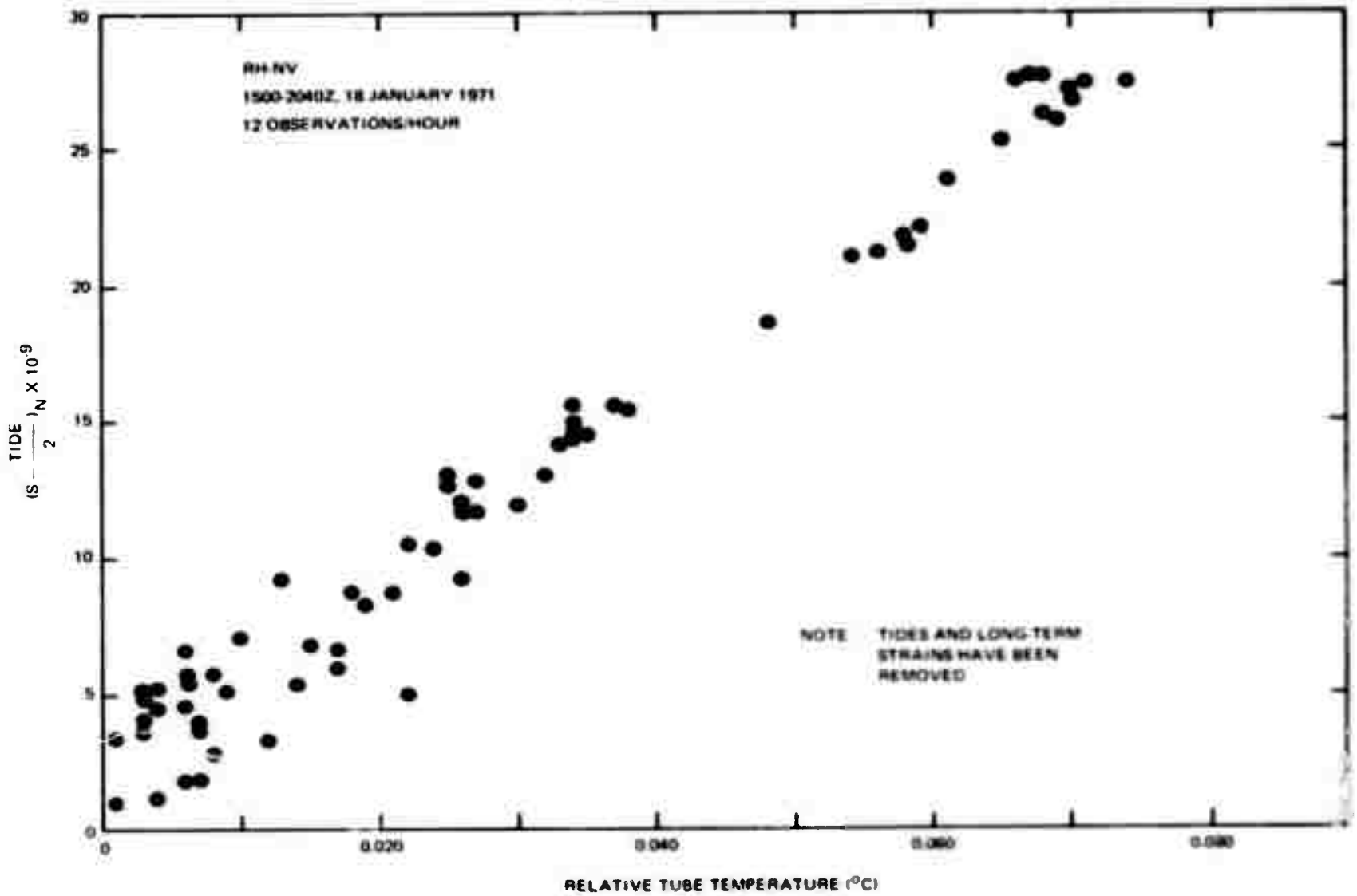

Figure 17. Scatter diagram of strain and tube temperature from observations at 5-minute intervals over a 6-hour time period at site RH-NV showing a short-term strain-temperature rate of 0.4×10^{-6}/°C.

G 6552

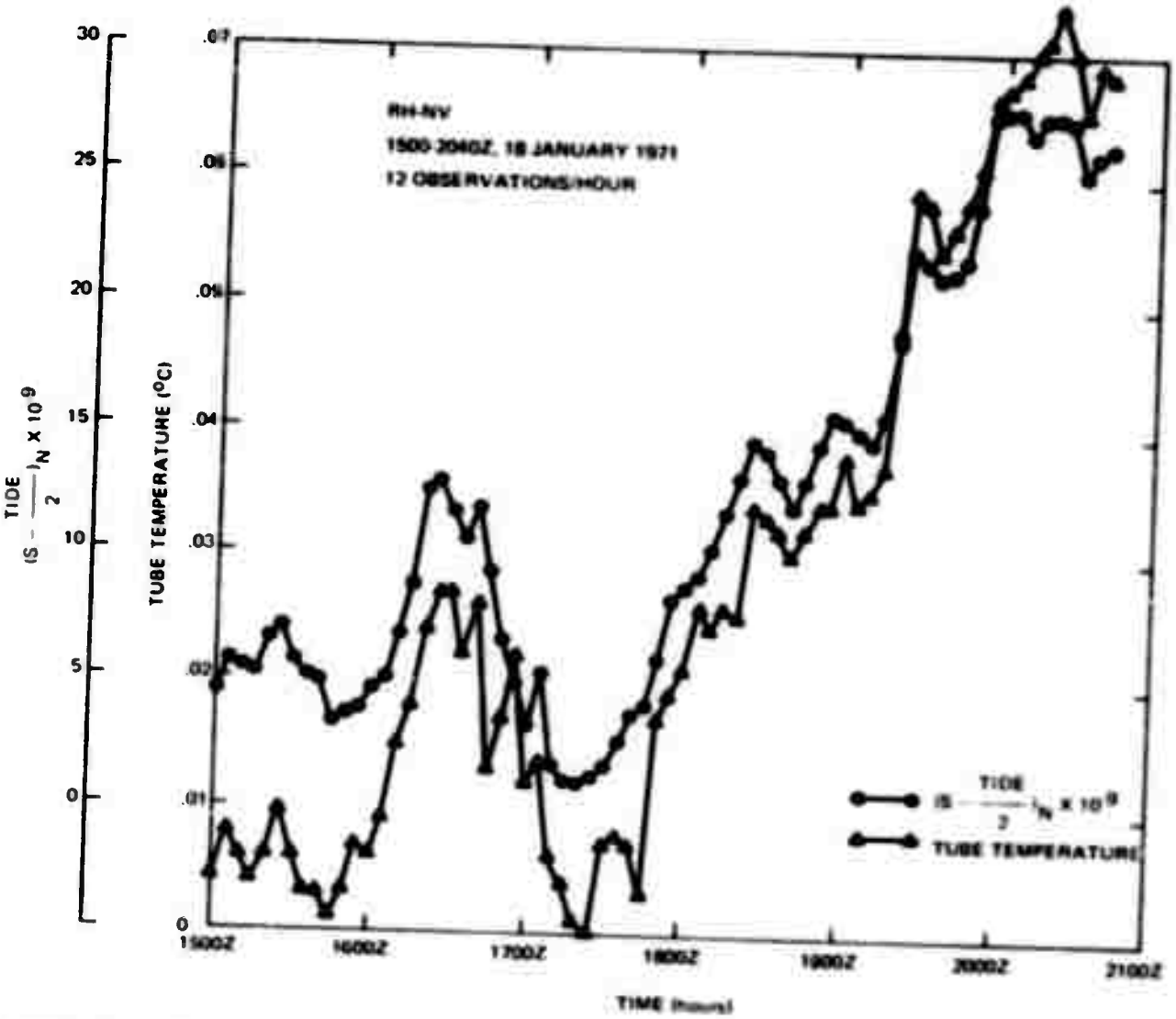

Figure 18. Strain and tube temperature from observations at 5-minute intervals plotted as a function of time.

G 6553

To test the feasibility of using tube temperature measurements to subtract temperature effects in order to determine the character of the decay of the strain step associated with large earthquakes and explosions, a predicted strain output was computed using the relationship

$$\Delta\delta_{PRED} = \frac{\Delta\delta_{TID}}{2} + [(6.5 \times 10^{-9}/HR) \times \theta] + 0.34 \times 10^{-6}/°C \times \Delta T_{TUBE}$$

where

$\Delta\delta_{PRED}$ = predicted change in strain in a given time interval θ

$\Delta\delta_{TID}$ = change in theoretical tidal strain

θ = time interval in hours

ΔT_{TUBE} = change in temperature of the tube in centigrade degrees.

Predicted strains were computed at 5-minute intervals for a 3-hour period following the original 6-hour period from which the short-term strain temperature rate was computed. As shown in figure 19 the predicted strain is within 1×10^{-9} of the observed strain for 30 minutes into the predicted time period. The maximum deviation is 4×10^{-9} in the first 1-1/2 hours. The maximum deviation in the period 1-1/2 to 3 hours dropped to 2×10^{-9}.

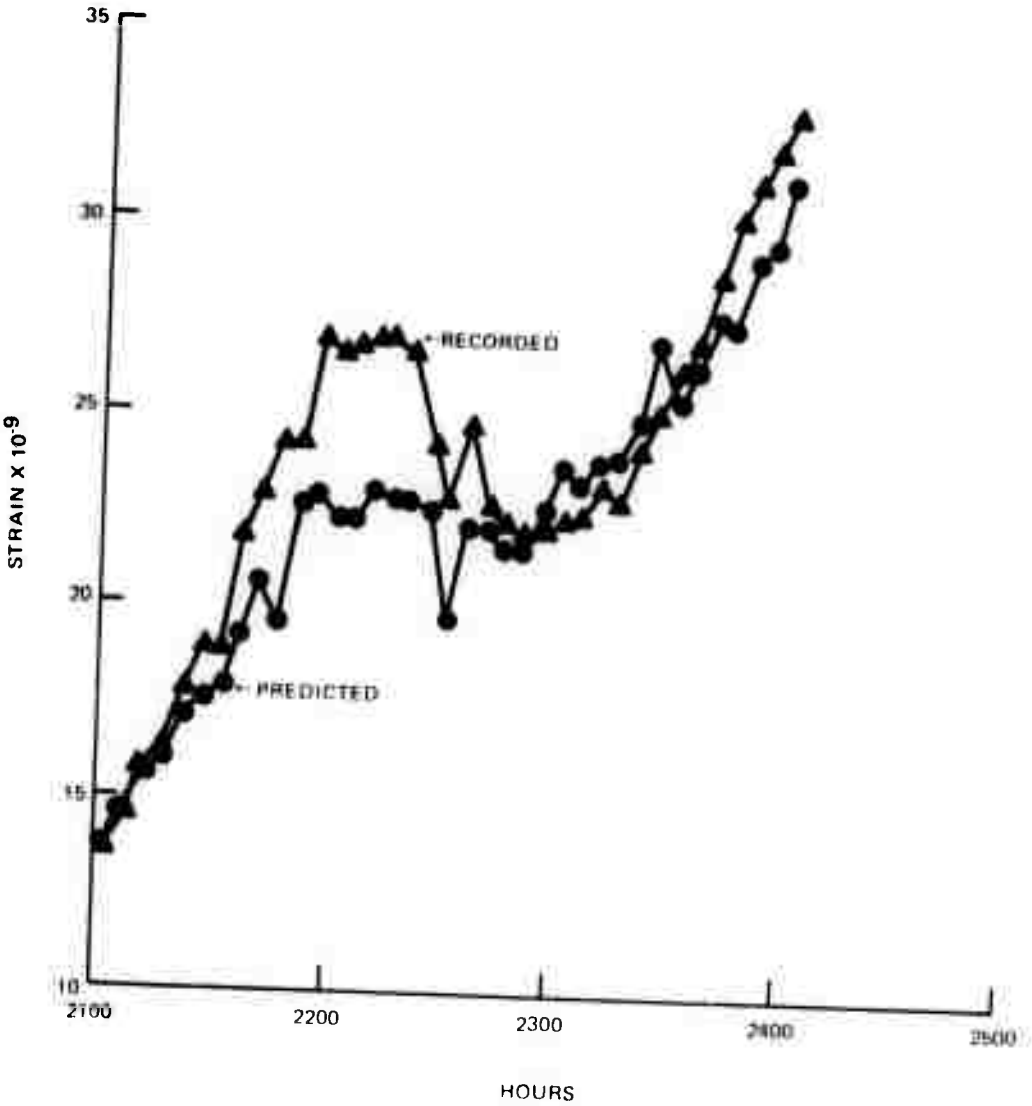

Figure 19. Recorded strain compared with predicted strain synthesized by applying strain-temperature relationships determined from measurements prior to the time period shown.

G 6554

5. CASE STUDIES OF SIGNIFICANT EVENTS

5.1 GENERAL

The analysis of explosion data has been limited to the following:

a. A comparison of the explosions CYATHUS and BANEBERRY, requested by the Project Office;

b. A report on the San Joaquin Valley earthquake, requested by the Project Office.

c. A case study of the NTS explosion MINIATA, demonstrating examination of a single event recorded at six sites.

d. A comparison of the character of the strain step of an earthquake and an explosion;

e. A study of the relation between direction of the strain step and changes in regional strain conditions.

5.2 EXPLOSIONS CYATHUS AND BANEBERRY

A report entitled "Preliminary Comparison of NTS Explosions CYATHUS and BANEBERRY" shown as appendix 2 of this report, was prepared at the request of the Project Office and forwarded on 14 January 1971. The data from the two events, which were of equal predicted yield and approximately the same epicenter, showed a factor of six larger ground amplitude from BANEBERRY than from CYATHUS as recorded at Queen Creek, Arizona, a distance of 618 km. In contrast, BANEBERRY produced about one-half as much earth strain at portable strain site YM-NV compared with QM-NV, both at an epicentral distance of approximately 50 km. Differences in the two explosions were also observed in the 1-minute rise time for CYATHUS (attributed to the rise time of the 0.01 sec filter in the system) and a 2-minute rise time for BANEBERRY.

Additional information from the short-period strain-inertial seismograph at Houlton, Maine (HN-ME) showed BANEBERRY to be clearly recorded at 1.0 Hz at a S/N ratio of 4, whereas no signal from CYATHUS was discernible at approximately the same background level.

5.3 THE SAN JOAQUIN VALLEY EARTHQUAKE OF 09 FEBRUARY 1971

Also requested by the Project Office was the report in appendix 3 entitled "Preliminary Notes on the San Joaquin Valley Earthquake of 09 February 1971 from Portable Strain Records," dated 19 May 1971. The main points of that report together with additional observations and conclusions follow.

Figures 20 and 21 show magnetic tape playback of the primary strain and the wide-band low-gain strain channels at sites YM-NV and QM-NV, respectively. It is noted that, fortuitously, the system sensitivities were ideal for recording a magnitude 6.2 earthquake from California. It is significant to note that the step at YM-NV occurs 15 to 17 seconds after onset of the Sg phase or approximately at the onset of the Rg phase. The principal step at YM-NV lasts 10 seconds longer than predicted by the filter response, and at QM-NV lasts 1 minute longer than predicted. It is possible that local strains are contributing to the duration of the step, or that the step is being triggered by more than one phase.

From table 8 the velocity of the strain step for QM-NV and YM-NV are in close agreement and compare favorably to the average velocity 3.0 ±0.3 km/sec reported by Wideman and Major (BSSA, Dec. 1967) for a continental path. The amplitude of the strain step at both QM-NV and YM-NV agree closely with Wideman and Major; whereas, the observed step is lower by a factor of 2.3 at TI-NV and higher by a factor of 1.3 at RH-NV.

Table 8. Observed amplitude and velocity of the strain step from the San Joaquin Valley Earthquake of 09 February 1971

Site	Observed amplitude of strain step	Amplitude of strain step from Wideman and Major	Observed step velocity (km/sec)
QM-NV	6.4×10^{-9} e	6.4×10^{-9}	3.06
YM-NV	6.5×10^{-9} c	6.6×10^{-9}	3.03
TI-NV	2.9×10^{-9} c	6.8×10^{-9}	
RH-NV	8.0×10^{-9} c	6.2×10^{-9}	

e extension
c compression

A plot of the strain step at YM-NV is shown as figure 22. The tide and long-term temperature trend have been removed. The effect of the filter is negligible about 100 seconds after the onset of the step. The step has a maximum quasi-static strain of 7.8×10^{-9}, an exponential decay with a 7-minute time constant, and a residual strain of 5.8×10^{-9}.

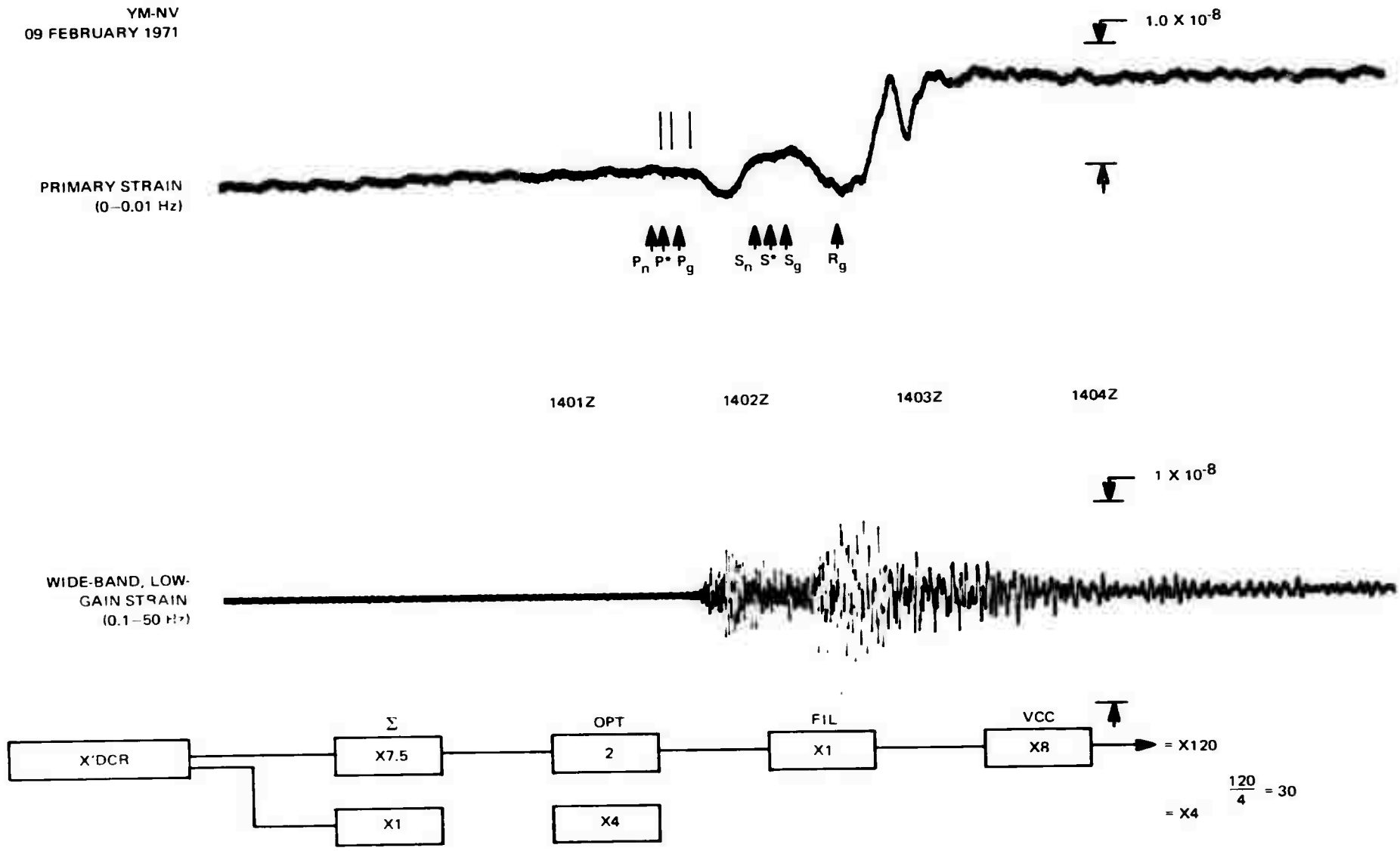

Figure 20. Magnetic tape playback of the primary strain and wide-band, low-gain strain channels at Site YM-NV showing the signal from the San Joaquin Valley earthquake of 09 February 1971. The step appears to occur at the onset of the R_g phase.

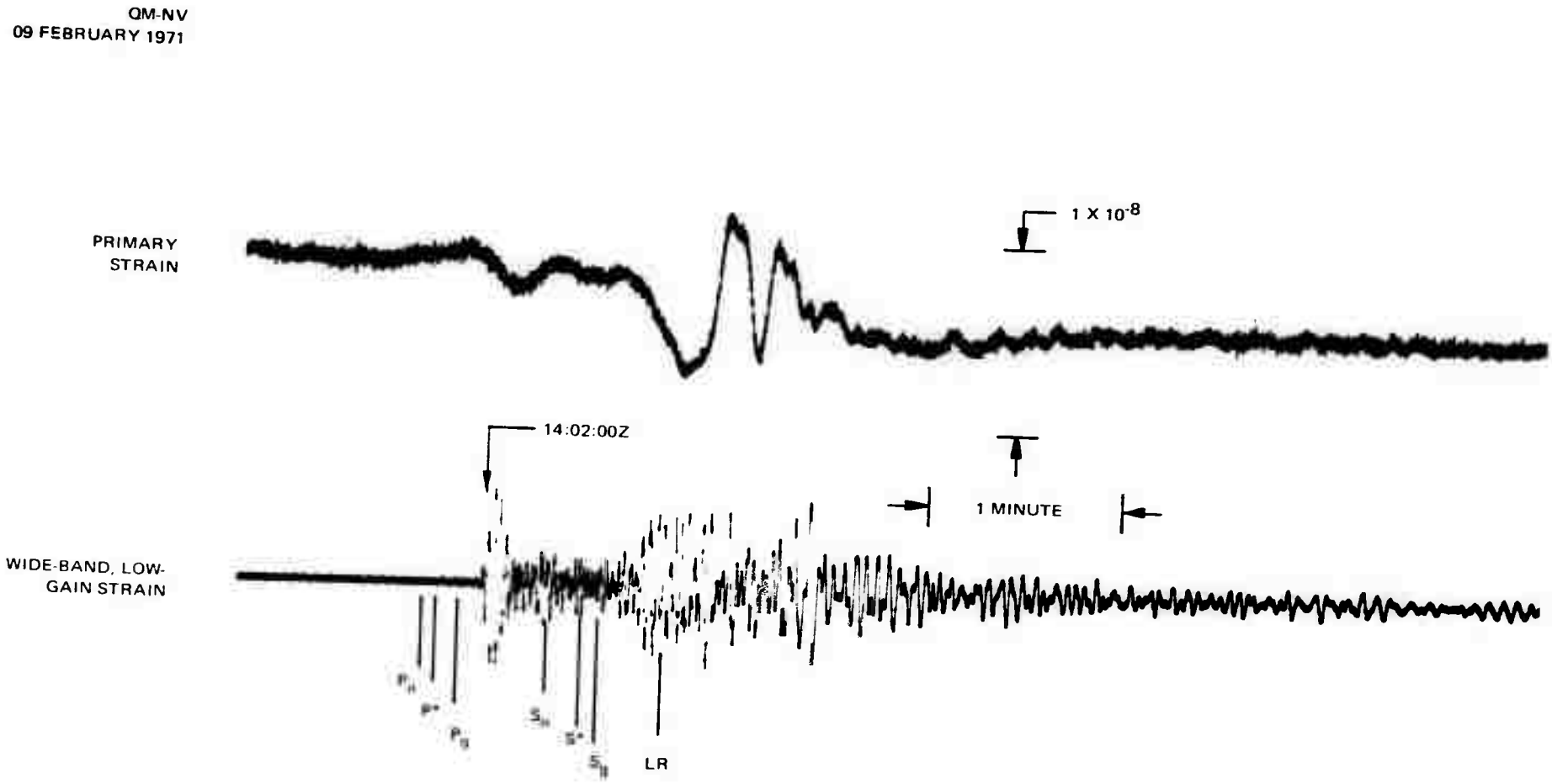

Figure 21. San Joaquin Valley earthquake recorded at Site QM-NV. The duration of the strain step lasts about one minute longer than at YM-NV and the step appears to have been triggered by more than one phase. $\Delta = 3.54°$.

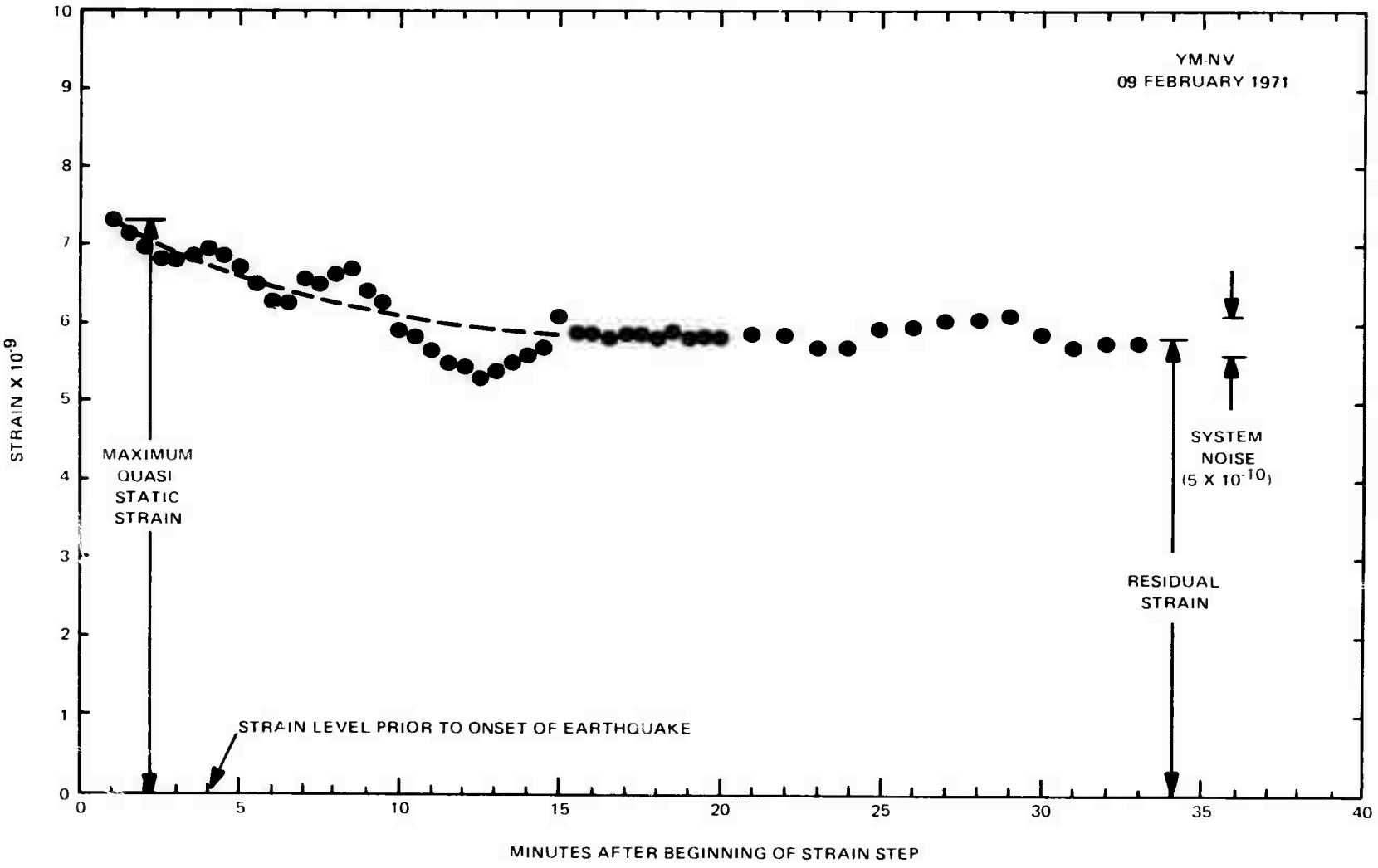

Figure 22. Strain step of San Joaquin Valley earthquake recorded at Site YM-NV replotted after removal of tide and secular strain.

G 6555

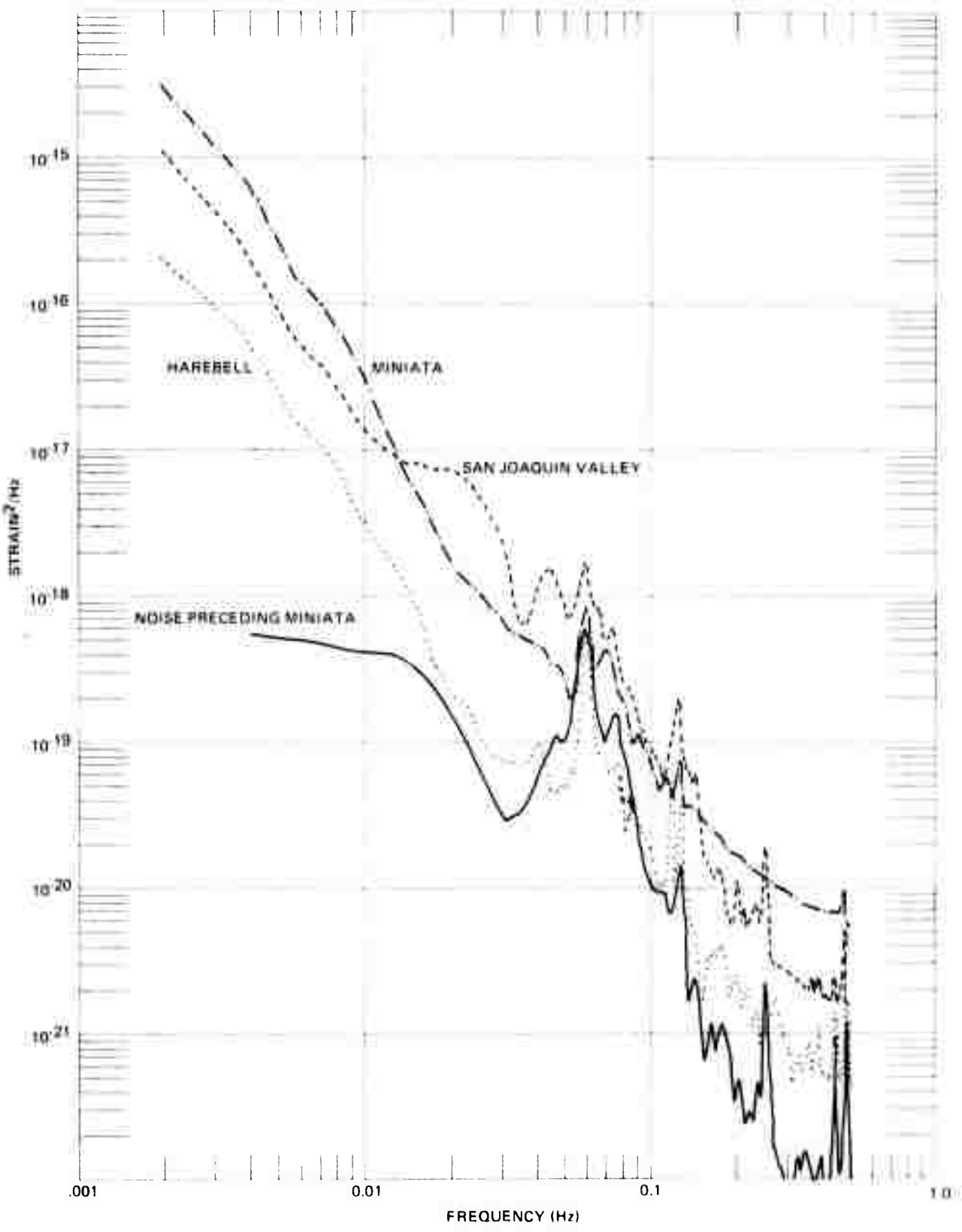

Figure 23. Power spectral density in strain^2/Hz of noise and signal recorded on the primary strain channel at YM-NV for 3 events in 1971. The response of the system is included. The Nyquist frequency is 0.5 Hz.

G 6556

Power spectral density plots of the San Joaquin Valley earthquake and two NTS explosions recorded at site YM-NV are shown for the primary strain channel in figure 23. The San Joaquin event which travels a greater distance to YM-NV contains less energy at high frequencies (0.1 to 0.5 Hz) than at lower frequencies (0.01 to 0.1 Hz) compared with the NTS events HAREBELL and MINIATA. Differences in direction of approach also probably contribute to the spectral distribution of the energy, since the strainmeter has a different azimuthal response to longitudinal than to transverse waves. Orthogonal horizontal strain instruments are required for proper analysis.

It is also indicated from figure 23 that the San Joaquin earthquake compared with HAREBELL and MINIATA has less strain at frequencies shorter than 0.01 Hz relative to the frequency range 0.01 to 0.1 Hz. Both distance and site coupling are factors which affect the comparison. The azimuth of approach and local strain conditions could also be contributing factors. The relative power levels of the three events at frequencies lower than 0.01 Hz are comparable with step strain measurements of 15×10^{-9}, 6.5×10^{-9}, and 3.6×10^{-9} for the events MINIATA, San Joaquin Valley, and HAREBELL, respectively.

5.4 CASE STUDY OF NTS EVENT 'MINIATA' of 08 JULY 1971

The event MINIATA of 08 July 1971 has been selected for a case study because it is recorded at all sites with a high signal-to-noise ratio. In fact, the signal at OB-NV exceeded the linear range of the summation amplifier. Power spectral density plots at all sites except OB-NV are shown for the primary strain channel in figure 24. The response of the system (channel No. 1 in figure 3) has not been removed. With single strainmeters at each site the influence of both angle of approach and distance on the spectral distribution of the site is again ignored. However, it is noted from the similarity of the curves in figure 24 that the spectral distribution of the signal is nearly equal among the sites at frequencies lower than 0.1 Hz - suggesting that the angle between the direction of approach of the signal and the axis of the strainmeter might not be an important factor at the longer periods. The curve for RH-NV does not match the other four because the signal at RH-NV is at the level of the noise.

Power plots for the wide-band hi-gain channel for MINIATA are shown in figure 25. A typical noise distribution for the five sites is shown in figure 26 which contains the signal and noise power plots for the wide-band hi-gain strain channel at site QM-NV. The data, which has a high signal to noise ratio at all frequencies between 0.08 and 10 Hz, contain an anomalous dip in the power curve of site RH-NV in the frequency range 0.2 to 0.7 Hz. To determine whether this anomaly was related to the apparent low coupling coefficient obtained at site RH-NV from measurements of Rayleigh waves from large distant earthquakes, power spectra of the wide-band hi-gain data were computed for the Chilean earthquake of 09 July 1971 as shown in figure 27. The low response in the region of 0.1 to 0.2 Hz is confirmed. A low response at frequencies below 0.07 Hz relative to frequencies above 0.25 Hz is also evident. The Chilean earthquake is at an angle that gives high response to Rayleigh waves at RH-NV and KP-NV and high response to Love waves at all sites except RH-NV.

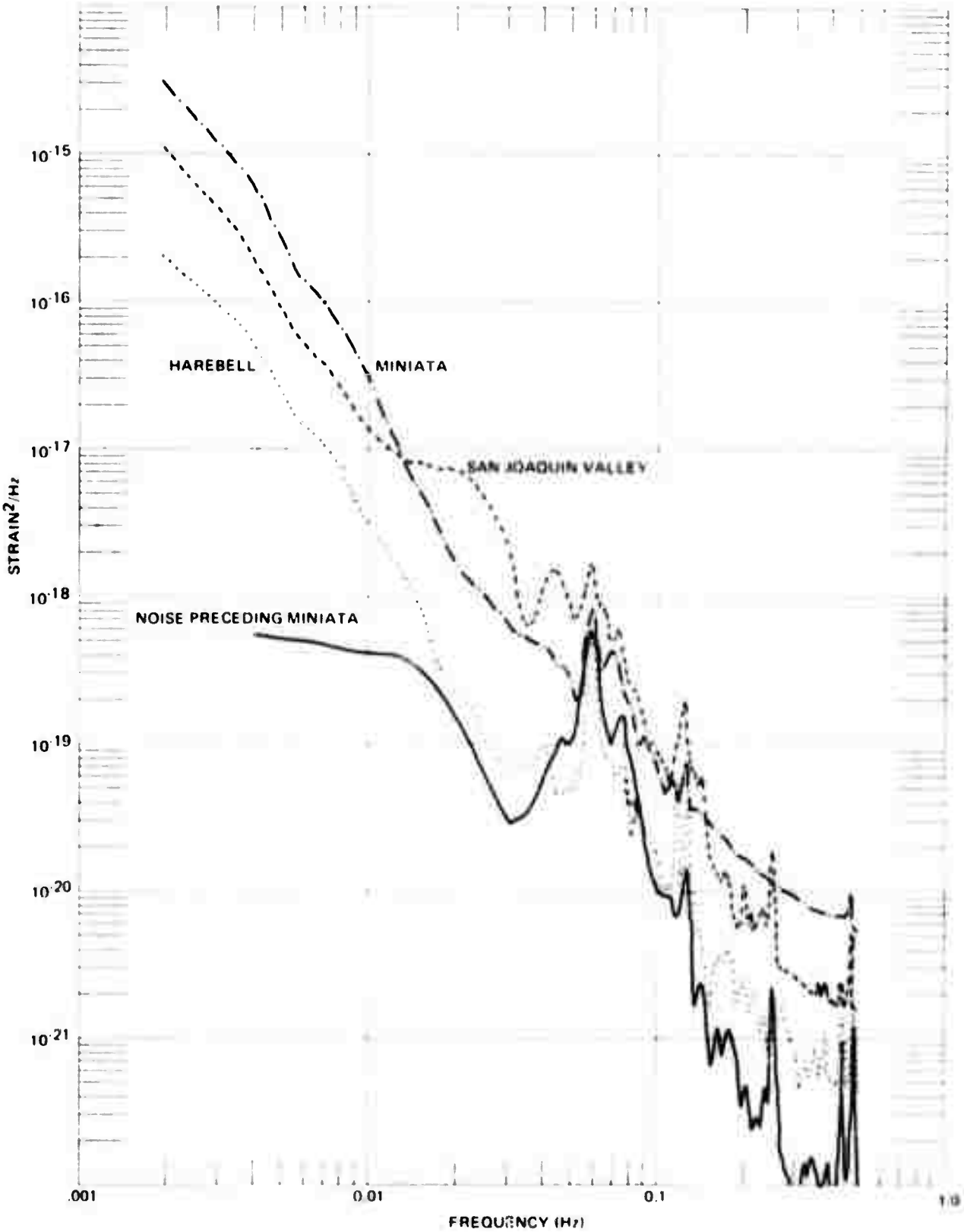

Figure 23. Power spectral density in strain^2/Hz of noise and signal recorded on the primary strain channel at YM-NV for 3 events in 1971. The response of the system is included. The Nyquist frequency is 0.5 Hz.

G 6556

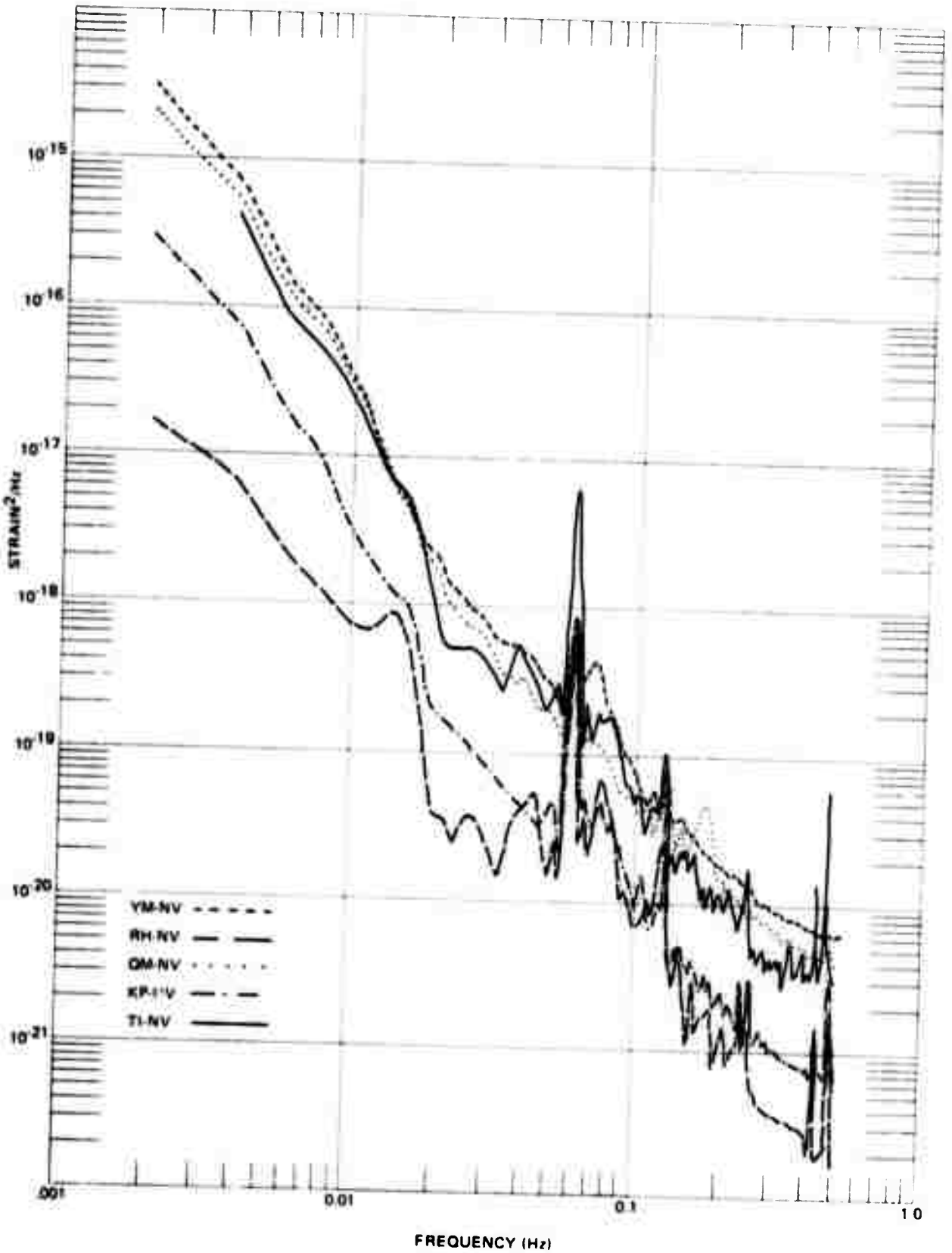

Figure 24. Power spectral density in strain^2/Hz of noise and signal for NTS event MINIATA recorded on the primary strain channel at 5 portable strain sites on 08 July 1971. The Nyquist frequency is 0.5 Hz.

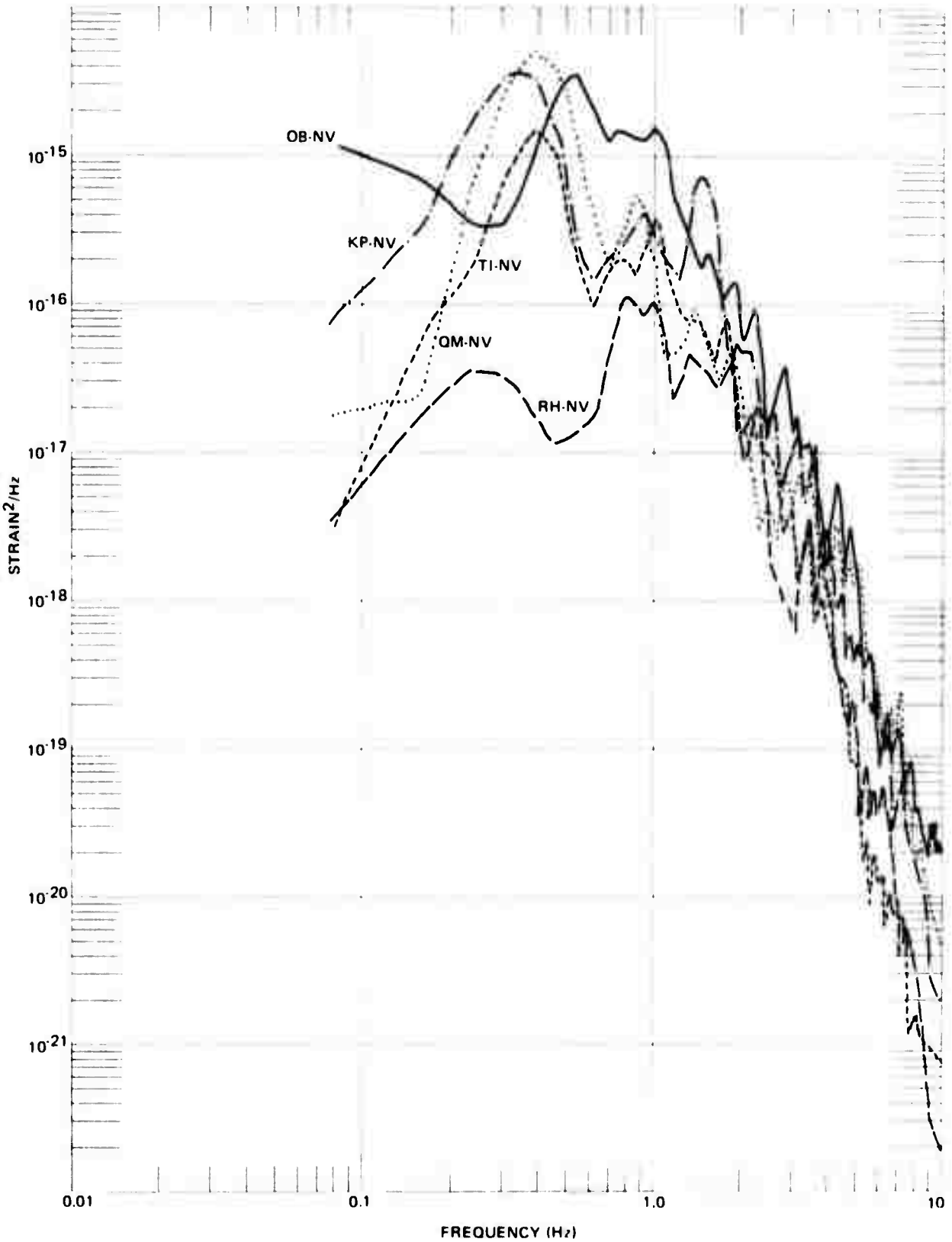

Figure 25. Wide-band high-gain strain plots of power spectral density in strain^2/Hz for the NTS event MINIATA recorded at 5 portable strain sites on 08 July 1971. The Nyquist frequency is 20 Hz.

G 6558

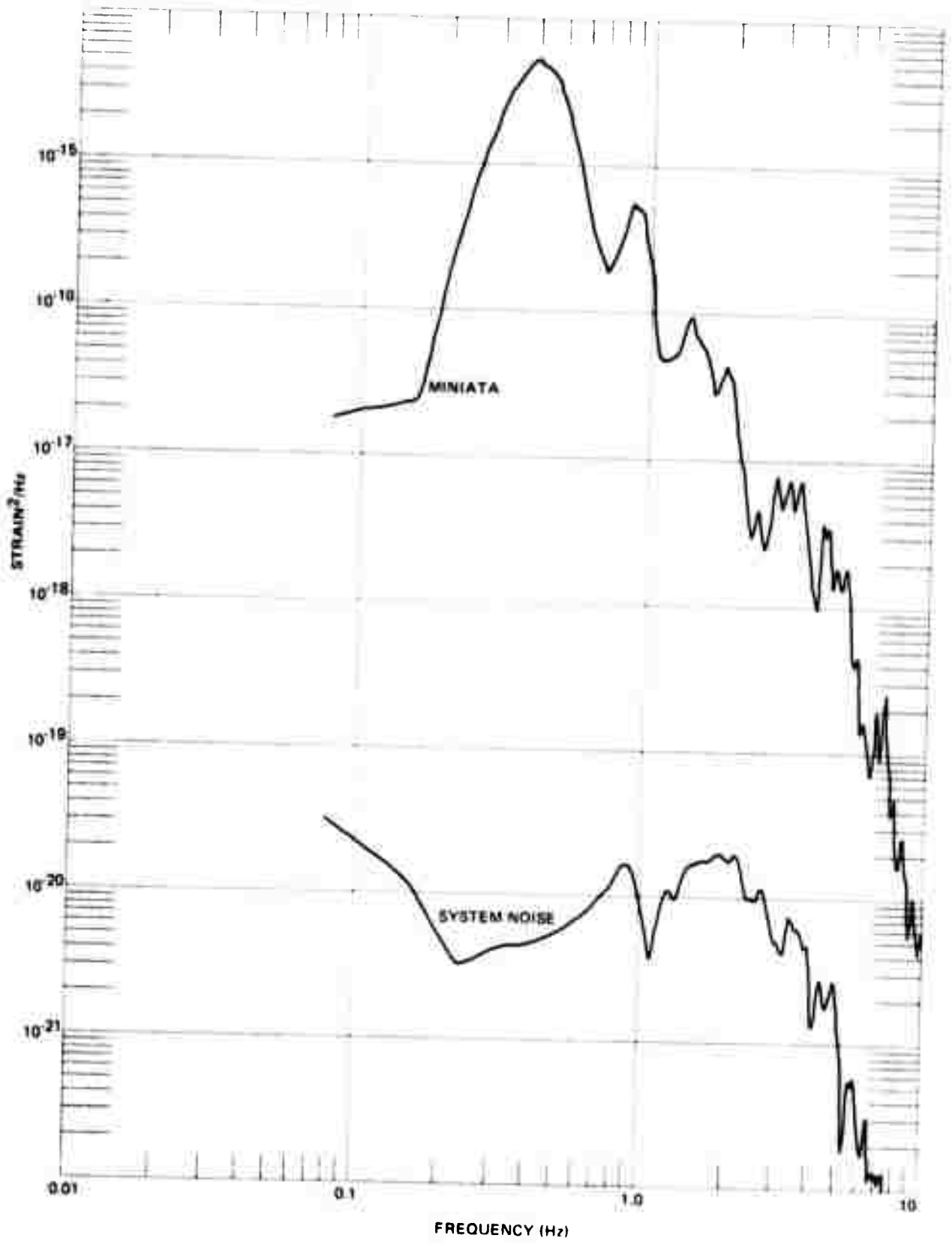

Figure 26. Power spectral density in strain^2/Hz for the MINIATA signal recorded on the wide-band high-gain strain channel at QM-NV. A plot of system noise at QM-NV which is typical of the 5 sites is also shown. The Nyquist frequency is 20 Hz.

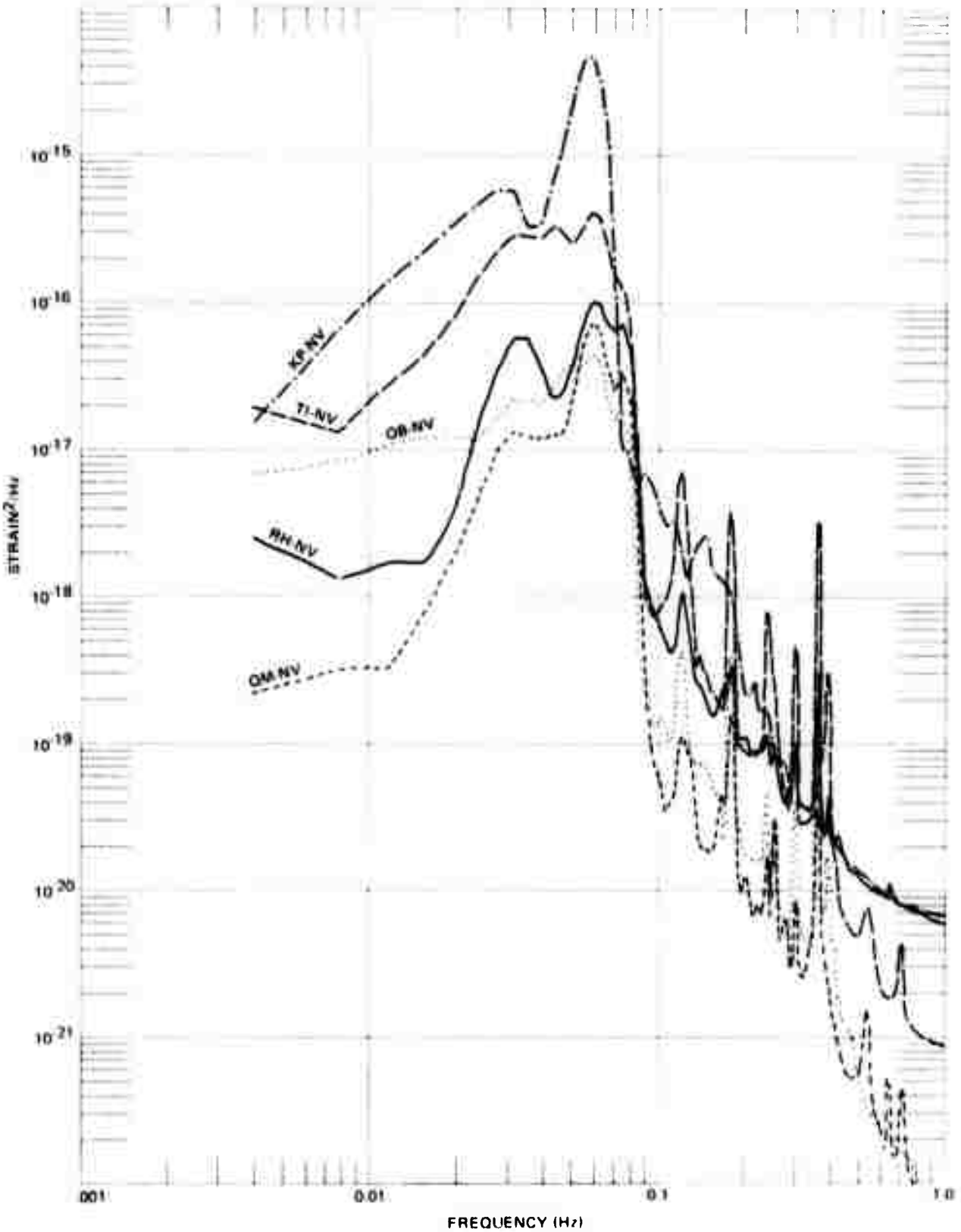

Figure 27. Wide-band high-gain strain power spectral density plots in strain^2/Hz for the Chilean earthquake of 09 July 1971 recorded at 5 sites. The Nyquist frequency is 1.0 Hz.

G 6560

However, for the MINIATA explosion the angle of approach to RH-NV and KP-NV are nearly equal and therefore should give the same response to Rayleigh and shear waves. Thus it appears that factors other than angle of approach are overriding.

The power curves for the Chilean earthquake (figure 27) have other interesting features. For one, it is observed that site coupling factors listed in table 5 in an earlier section of this report, obtained from measurements of the predominant 17-20 second Rayleigh waves, would give a higher coupling to site QM-NV and a lower coupling to site OB-NV if other frequencies in the wave train were used. It is important to note that the angle of approach to the strainmeter is nearly the same for sites QM-NV, TI-NV, and OB-NV; therefore, the relative energy of Rayleigh and Love waves can be ignored. It is also noted that at frequencies below approximately 0.015 Hz in figure 27, the power level for RH-NV and TI-NV is increased by system noise. However, the high level for the OB-NV curve occurs at a signal-to-noise ratio of 10 and therefore is not a spurious occurrence. It appears that relative power measured at 0.025 Hz (40 seconds) would lead to more representative values of relative coupling.

5.5 COMPARISON OF THE STRAIN STEP FROM AN EARTHQUAKE AND AN EXPLOSION

A comparison of the character of a strain step from an explosion and an earthquake is facilitated by the occurrence of a magnitude 4 earthquake (figure 28) at an epicentral distance of 40 km from QM-NV at 1952Z on 23 July 1970, followed 193 minutes later by the magnitude 5.5 NTS explosion SHAPER (figure 29) at an epicentral distance of 59 km from QM-NV. (Epicentral data were obtained from the Bulletin of the Seismological Laboratory, University of Nevada, July 1970). A time constant of 13 minutes for the earthquake compares with a time constant of 24 minutes for the explosion. The estimated amplitude of the strain step is 20×10^{-9} in compression for the earthquake and 49×10^{-9} in compression for the explosion. The maximum possible permanent offset, if any, is 7×10^{-9} for the earthquake and 10×10^{-9} for the explosion. The strains were corrected for the tidal trend and the daily temperature trend; however, short-term temperature effects were not correctable at QM-NV in March 1970.

5.6 TRENDS IN DIRECTION OF STRAIN STEP

A study of regional strain trends is beyond the scope of the current contract. Nevertheless, even a cursory examination of the direction of the strain step allows some significant conclusions to be drawn. A few prefactory remarks relating to the term "strain step" are in order at this point. The term "strain step" as used in this report refers to the change in strain (compression or extension) associated with the arrival of surface waves from earthquakes and explosions. No attempt is made to either confirm or deny the existence of a propagating strain step, evidence for which was reported by Wideman and Major (1967). The existence of only one component at a station precludes any attempt to measure the rate at which strain steps decay with distance, a subject of debate discussed by Romig, et al (1969). The explosion

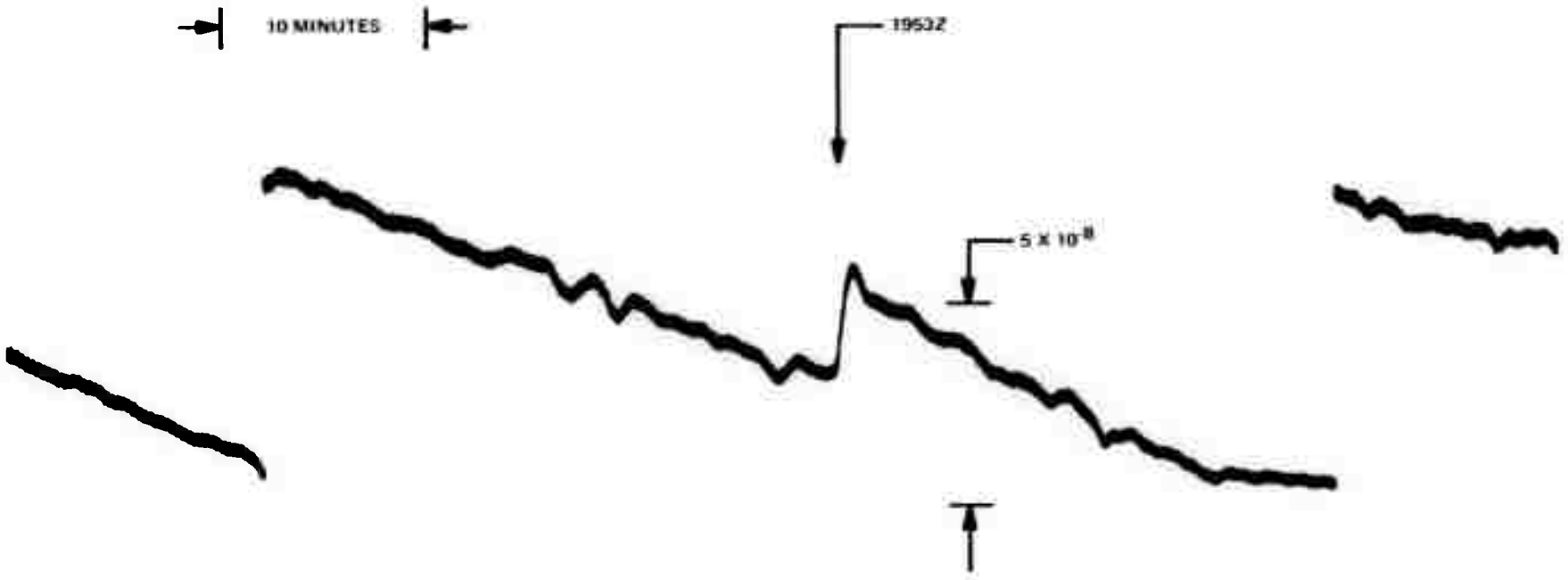

Figure 28. Magnitude 4 earthquake recorded at site QM-NV on 23 March 1970. Origin time 19:52:13.1Z; 37.817N 116.068W; Mag. 4; Δ=40 km.

G 6561

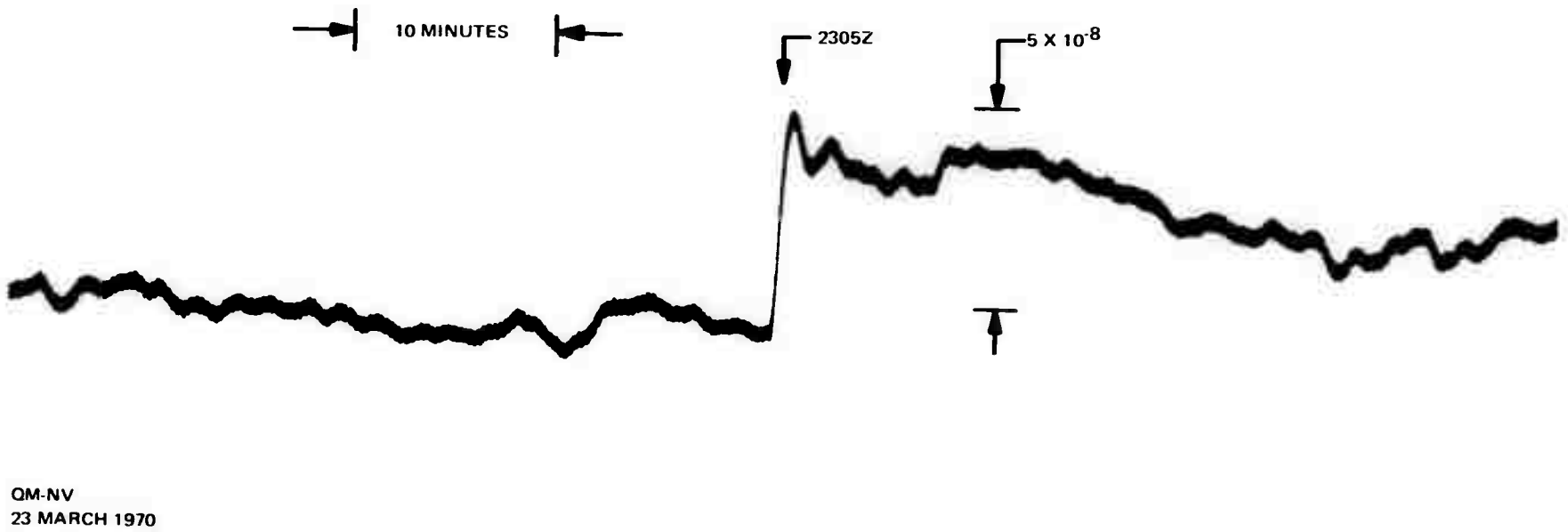

Figure 29. Magnitude 5.5 NTS event SHAPER recorded at site QM-NV on 23 March 1970. Origin time 2305Z; 37.086N 116.021W; Mag. 5.5.

G 6562

data presented here shows that if a propagating strain step does exist, it is masked by strain offsets that are clearly not caused by mechanical hysteresis in the instruments. Specifically, the data show strong evidence that the strain offsets are a result of local release in the vicinity of the strainmeter, an effect discussed by Smith, et al (1969) and supported by Boucher, et al (1971), based on a comparison of strain offsets from explosions and associated cavity collapses. The results also tend to support tentative conclusions drawn by Smith and Kind (1971) relating observed strain changes to regional tectonic stresses. We can build an argument for the predominance of local strain release from the data in table 9, which lists the direction, compression (+) or extension (-), of the quasi-static strain from 25 NTS explosions recorded in Southern Nevada in the period January 1970 through July 1971. Included in table 9 are two local earthquakes and the San Joaquin Valley earthquake of 09 February 1971. Noting that all explosions listed in table 9, except HANDLEY, are located in area B in figure 9, a nearly fixed azimuth angle from station to epicenter can be assumed for all of the listed explosions. It follows that despite the availability of only one strainmeter at each site a comparison of the direction of strain offsets provides meaningful results without computing the strain ellipse. A definite chronological grouping of the direction of the strain step is observed in table 9. Specifically, we note that a pattern of consistent direction of the step, persisting for at least a 9-month period is interrupted by a directional change at each site between late December 1970 and early in 1971. In this period, steps changed from compressional to tensional at sites QM-NV, TI-NV, YM-NV, and OB-NV, and from tensional to compressional at sites RH-NV and KP-NV. Whether the occurrence of the San Joaquin Valley earthquake in the same time period is significant is a moot question. However, major changes in the strain field in Southern Nevada in December 1970 and January 1971 as reported by Smith and Kind (1971) and an apparent change in the trend of secular strains at 4 of the 6 sites for a period of several days preceding the San Joaquin Valley earthquake of 09 February 1971, as shown in figure 5, bear further investigation.

The data of table 9 have been replotted schematically in figure 30 in terms of a very approximate relative amplitude of the recorded signal to provide a coarse measure of the reliability of the estimated direction of trace offset. Referring now to the data for site OB-NV, we note that within a period of a few weeks, a reversal of the strain offset occurs between events HAREBELL on 24 June 1971 and MINIATA on 08 July 1971. The estimated direction is obviously reliable since figure 30 indicates that both signals were well recorded. Furthermore, if we compute the station-to-epicenter azimuthal angle for the two events, we find that the angles differ by only 9 degrees. Seasonal effects are ruled out as a contributing factor.

Perhaps of some significance is the fact that two local earthquakes (one, a magnitude 4 event occurring 40 km northeast of QM-NV at 19:52:13.1Z on 23 March 1970, and the other, an event occurring within 10 km of QM-NV at 1922Z on 06 July 1971), produced offsets in the same direction as for concurrent explosions. Furthermore, strain offsets from the San Joaquin Valley earthquake did not differ in direction from the previous recorded explosion at a given site, which tends to further substantiate the hypothesis that the direction of the strain step is controlled by local stress readjustments induced by the dynamic loading of the seismic waves.

Table 9. Summary of direction of strain steps measured at portable strain sites for events from January 1970 through July 1971

Date	Event	Site					
		RH-NV	KP-NV	QM-NV	TI-NV	YM-NV	OB-NV
01/23/70	FOB	0				0	
01/30/70	AJO	0					
02/04/70	GRAPE B	+		+			
02/05/70	LABIS	0		0			
02/11/70	DIANA MIST	-	0	+			
02/25/70	CUMARIN	0	0	0		+	
02/26/70	YANNIGAN	0	-	0		+	
03/06/70	CYATHUS	0	-	-		-	
03/06/70	ARABIS	0	-	0		0	
03/19/70	JAL	0	-				+
03/23/70	MAG 4 QUAKE		0	+	0	0	
03/23/70	SHAPER		0	+	+	+	+
03/26/70	HANDLEY	-	-	+	+	+	+
04/21/70	SNUBBER		0	0	0	0	+
04/21/70	CAN		0	0	0	0	+
05/01/70	BEEBALM						+
05/01/70	HOD						+
05/05/70	MINTLEAF						+
10/14/70	TIJERAS	-		0	+	+	+
11/05/70	ABEYTAS	0	0	0		+	+
12/06/70	ARTESIA		-	+	+	+	+
12/17/70	CARPETBAG	+	-	+	+	+	+
12/18/70	BANEBERRY	0	0	-	0	+	+
02/09/71	SAN JOAQUIN	+		-	+	+	
06/23/71	LAGUNA	0		0	0	-	-
06/24/71	HAREBELL	0	+	+		-	-
07/06/71	LOCAL QUAKE	0	+	+	0	0	0
07/08/71	MINIATA	+	+	+	-	-	+

+ compression
- extension
0 - no discernible step
blank - no data

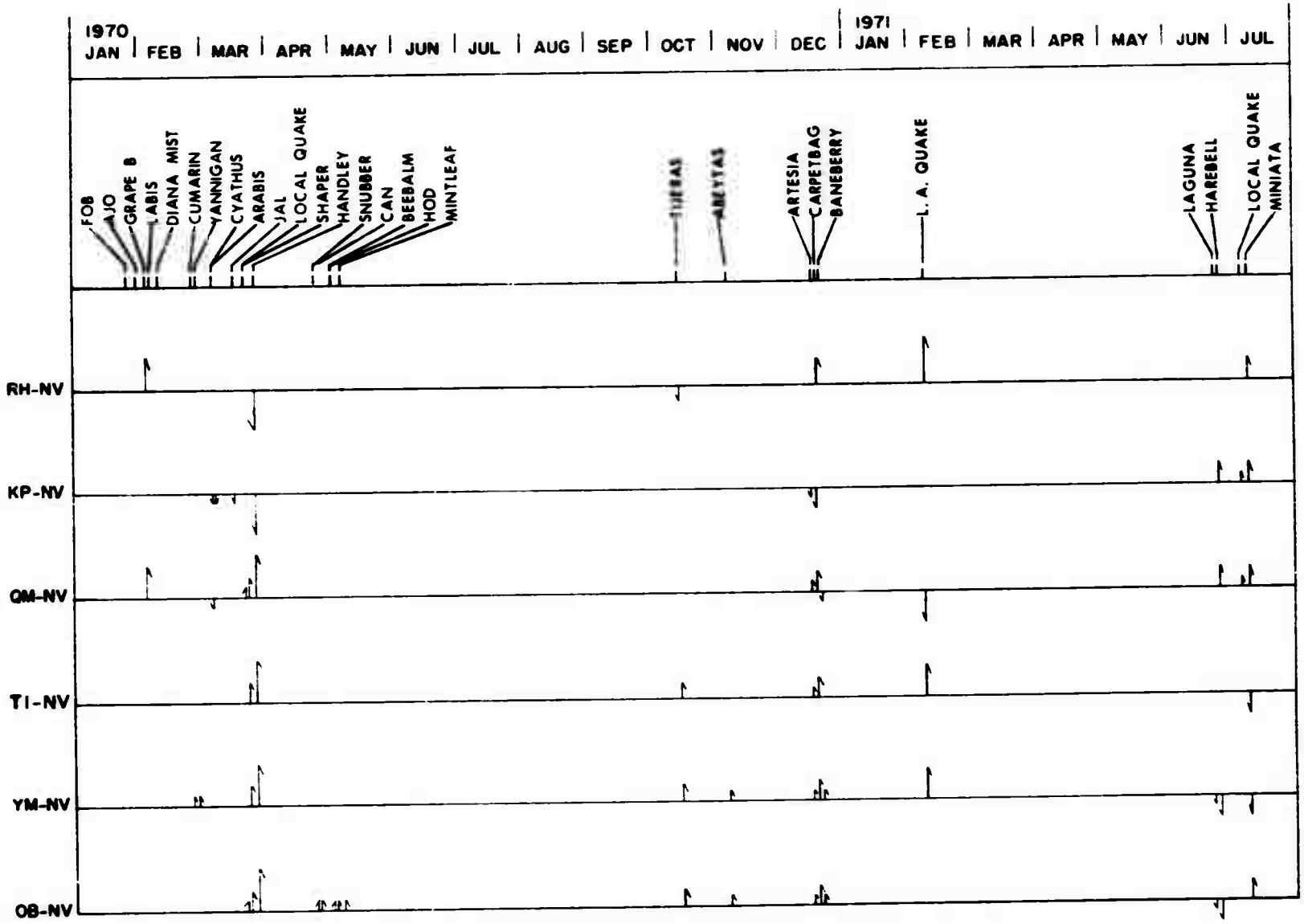

Figure 30. Chronological plot of approximate relative amplitudes of recorded strain step for the events listed in table 9.

G 6572

It is also interesting to note that a strain step was observed at site QM-NV at the time of arrival of both the body waves and the surface waves for both the San Joaquin Valley earthquake (figure 21) and the local earthquake of 06 July 1971. The phenomenon of a double strain step was also reported by Wideman and Major (1967).

6. CONCLUSIONS

6.1 STRAIN STEPS

This report presents new information supporting the hypothesis that dynamic loading by the seismic waves from explosions and earthquakes trigger a local release of tectonic strain (a strain step), and that trends in the direction of strain steps appear to be related to regional tectonic strain.

This hypothesis is supported mainly by five factors:

1. The direction of the strain steps at any one site show chronological patterns that are clearly not related to seasonal effects.

2. Long-term trends in the direction of the strain steps at a given site change without corresponding changes in general epicenter location and yield of the explosions.

3. Chronological patterns of the direction of the strain steps appear to be independent of type of event (explosion or earthquake), and independent of size, distance, or azimuth of approach of the events.

4. Trends in the direction of the strain steps among the six sites appear to be chronologically related.

5. A major change in the rate of change of secular strain occurred at several sites in January and February 1971, nearly coincident with changes in direction of explosion-induced strain steps at all sites.

6.2 COUPLING OF EARTHQUAKES AND EARTH TIDES

Pronounced differences are observed among the six portable strain sites in relation to the degree of coupling of the instruments to the surface rock or of the surface rock to the rock at depth. The relative coupling factors among the six sites show the same relationship for earth tides as for earthquakes. Low coupling factors for both sites RH-NV and OB-NV could be related to the fact that both sites are located in sharp ridges - the only apparent geological feature that is common to both sites yet is absent at the other four.

6.3 THE RELATIVE MERIT OF TRENCH AND TUNNEL INSTALLATIONS

As strain data from trench and tunnel installation are compared, together with a consideration of site selection problems, several appealing features of trench installations come into focus. In particular, the use of trenches does not restrict the selection of sites to locations containing existing excavations, as occurs with the use of mine tunnels. Therefore, more accessible locations are available, and there is greater freedom in the selection of rock conditions, topographical features, and orientation of

the strainmeter. In regard to environmental effects, pressure-induced strains appear to be less prevalent; the secular strain over the annual cycle returns nearly to its original position; and the coupling factor for earthquakes and earth tides was relatively high at both trench sites, in contrast with an abnormally low coupling factor at 2 of the 4 tunnel sites.

6.4 PREDICTION OF STRAIN

It has been shown that tidal strains and temperature-induced strains at site RH-NV can be removed from the data to study the decay characteristics of step strains. However, the procedure was very time consuming and was successfully applied to data from the winter season only. The process will be equally complex at other sites because of the existence of complex combinations of long-term and short-term temperature and atmospheric pressure effects, and because of the need for more precise determinations of tidal coupling factors.

6.5 CASE STUDIES

The analysis of explosion data is limited by the availability of only one strainmeter at each site. In addition, the conclusions to be drawn are limited to the results of four case studies, each of which bears little or no direct relation to the other because of their divergent objectives. Nevertheless, three interesting results, among several, are noted.

A case in point is the 1-minute time difference in the rise time of the strain-step from the CYATHUS and BANEBERRY explosions recorded at QM-NV, 9 months apart, and a 50-second time difference in the rise time between recordings of the step at sites QM-NV and YM-NV for the San Joaquin Valley earthquake of 09 February 1971. These data suggest that the rise time of the step is more strongly influenced by tectonic conditions at the recording site than by source conditions, at least for epicentral distances and event magnitudes considered here.

In the case study of NTS event MINIATA, representing an event recorded at a different distance and angle of approach among the six sites, the spectral distribution of the signal was found to be nearly equal among the sites at frequencies lower than 0.1 Hz. These results suggest that the angle between the direction of approach of the signal and the axis of the strainmeter is not an important factor at the longer periods. It is not understood why this is so.

The case study of CYATHUS and BANEBERRY revealed interesting results aside from the unexpected high yield from BANEBERRY. It is not obvious why BANEBERRY was recorded at substantially greater ground amplitude than CYATHUS by inertial seismographs, yet at much less strain amplitude. Here again the hypothesis that local stress release is the predominant factor, seems plausible.

7. RECOMMENDATIONS

7.1 GENERAL

The analysis of the strain records for this project has consisted mainly of the reduction of data, the development of analysis techniques, the cursory examination of data trends, and the completion of a few case studies of significant events. A detailed follow-up study using existing recordings is recommended. Such a study would contribute greatly to an understanding of the relation between such parameters as regional-strain and weather-induced phenomena; theoretical and apparent tidal strains; the direction of the step strain from events and regional or local strain conditions; spectral distribution of energy from events and factors such as distance, type of source, and site conditions; rise time of the strain step and source factors; duration of the strain step and source type; and duration of the strain step and site conditions. More important is the fact that a more detailed and thorough study of the aforementioned relations will provide a more accurate assessment of the limitations of near-surface strain installations for the study of regional strains, tides, and near earthquakes and explosions.

7.2 COUPLING OF THE TIDES AND EARTHQUAKES

The ratio of recorded tides to theoretical tides among sites are in approximate agreement with relative coupling factors determined from large earthquakes. The possibility has not been ruled out that anomalies exist in tidal strain patterns and/or the response to traveling waves. Additional measurements of earthquake coupling and refinement of existing data should be done. Sites RH-NV and OB-NV have the lowest coupling in response to both earthquakes and tides. Only a cursory comparison of geological features has been made in attempting to explain the low coupling factors. A more rigorous study is recommended.

7.3 PREDICTION OF STRAIN

In order to study the decay characteristics of strain steps, the degree of coupling of the earth tides must be determined more precisely, and strain-temperature relationships must be investigated further. The relation between observed and theoretical tides should be determined more accurately by treating a larger data sample and by determining the environmental effect more precisely. Techniques such as measuring the temperature effect at tidal zeros and tidal effects at equal temperatures were started late in the program. Optimum filtering of the environmental effects has not been done. Filtering to separate the semidiurnal tide from the diurnal tides and diurnal temperature effect has not been done either. It is recommended that these techniques be explored in order to improve the interpretation of the data.

7.4 SECULAR STRAINS

There appear to be no reliable criteria for predicting the response of the four tunnel sites to the environment; however, of the two trench sites, the deeper of the two (YM-NV) showed much less diurnal and seasonal change in strain than the shallower one (TI-NV). Much useful information relating to secular strain has not been analyzed. Information on the phase relation of secular strain and temperature as well as short-term strain and temperature have not been applied. Preliminary measurements show phase relations that differ markedly among sites. It is recommended that these data be analyzed since it could help solve questions concerning residual strains over the annual cycle.

7.5 RISE TIME OF STRAIN STEP

Very little analysis of the character of the dynamic phase has been done in this report period. The rise time of events can be determined by removing the filter response of the primary strain channel. The decay character of many of the strain steps still have not been measured. Many low yield events recorded at site OB-NV are available for analysis. It is recommended that these important features of the signal be studied using existing recordings.

7.6 DECAY OF STEP

Analysis of the amplitude and duration of the step and categorizing the results by yield, by site, and by distance remains to be done.

7.7 AMPLITUDE OF STEP

The amplitude of the quasi-static strain step has been measured only for isolated case studies. It is recommended that amplitude measurements be made for the 70 steps in table 9 for which direction of the step has been ascertained, and that these amplitudes be related to source energy. Amplitude data will also possibly support the hypothesis that the character of the strain step at a recording station is affected mainly by the local release of tectonic strain triggered by the dynamic loading of the seismic waves from an event.

7.8 COMPARISON OF SPECTRA OF EVENTS

The need for orthogonal horizontal strainmeters oriented at 45° intervals at each site to obtain omnidirectional responses to Rayleigh and Love waves and to enable the measurement of changes in the strain ellipse cannot be over-emphasized. With the existing single-component data, events must be grouped by angle of approach to the strainmeter axis as well as the usual consideration of magnitude and distance, in order to isolate spectral strain anomalies. Such an analysis can be performed using all of the existing data. The spectral

analysis presented in this report only demonstrates the approach to the analysis of individual events and does little to establish trends in the events. The spectral data also can be presented in a more usable form. For example, the primary strain and wide gain channels should be combined and the response of the system removed. Future instrumentation should include a channel that is flat in the frequency range 0.01 to 0.1 Hz.

7.9 AUXILIARY INSTRUMENTS

Accelerometers and inertial seismographs were part of an auxiliary system operated at site RH-NV from May through July 1971. The accelerometers were too insensitive to obtain useful recordings of low and low-intermediate yield explosions at the distances involved (100-120 km) to use in a survey of step strain amplitude as a function of incident energy. Where the inertial seismographs would have been useful for low and low-intermediate yield explosions, the portable strains were not operating at optimum sensitivity, and when large magnitude earthquakes were useful in strain coupling studies, the signals on the inertial seismographs at RH-NV were clipped. An optimum distance range for auxiliary inertial instruments in support of portable strain measurements for low and low-intermediate yield events is about 20-40 km.

7.10 TRENCHES VERSUS TUNNELS

The relative merits of tunnels and trenches as discussed in section 6.3 show clearly the advantages of trench sites. The reaction of tunnel sites to temperature changes not exceeding diurnal periods in length has not been examined in detail sufficient for reporting of the results. However, it is evident that trench sites, despite their close proximity to the surface, appear to be as stable as tunnel sites. Benioff (1959) points out that on flat earth, surface temperature variations produce stress variations at depth, but little or no strain increments. The fact remains, however, that the short-term strains bear no simple relationship to the measured temperatures. Therefore, it is recommended that more advanced analysis techniques be applied to existing trench data, particularly in view of the advantages noted for the use of trenched strainmeter installations.

8. REFERENCES

Benioff, H., 1959, Fused-quartz extensometer for secular, tidal, and seismic strains, Bull. Geol. Soc. Amer., vol. 70, p. 1019-1032

Boucher, G., S. D. Malone, and E. F. Homuth, 1971, Strain effects of nuclear explosions in Nevada, Bull. Seis. Soc. Amer., vol. 61, no. 1, p. 55-64

Capon, J., 1970, Analysis of Rayleigh-wave multipath propagation at LASA, Bull. Seis. Soc. Amer., vol. 60, no. 5, p. 1701-1731

Romig, P. R., M. W. Major, C. J. Wideman, and D. Tocher, 1969, Residual strains associated with a nuclear explosion, Bull. Seis. Soc. Amer., vol. 59, no. 6, p. 2167-2176

Smith, S. W., C. B. Archambeau, and W. Gile, 1969, Transient and residual strains from large underground explosions, Bull. Seis. Soc. Amer., vol. 59, no. 6, p. 2185-2196

Smith, S. W. and Kind, R., 1971, Regional secular strain fields in Southern Nevada (in press)

Wideman, C. J., and Major, M. W., 1967, Strain steps associated with earthquakes, Bull. Seis. Soc. Amer., vol. 57, no. 6, p. 1429-1444

APPENDIX 1 to TECHNICAL REPORT NO. 71-20

STATEMENT OF WORK TO BE DONE

STATEMENT OF WORK TO BE DONE

VELA T/0703/B/ASD(32)

Amendment No. 4

18 September 1970

d. Expansion and Extension of Special Projects Actions. Certain actions initiated and conducted under Tasks a, b, and c above require extension of the time period originally provided and of the level of effort as follows:

"(1) Operation of the six existing and installed strainmeter systems initiated during Aug 1970 is to be continued through the project period. Continuous data recording and subsequent analysis of long-term environmental effects observed during this period is required. Detailed interpretations of strain data obtained from significant individual events are required at a rate of approximately one event per month to be selected as data are collected or as specified by the Government."

APPENDIX 2 to TECHNICAL REPORT NO. 71-20

PRELIMINARY COMPARISON OF NTS EXPLOSIONS CYATHUS AND BANEBERRY

PRELIMINARY COMPARISON OF NTS EXPLOSIONS CYATHUS AND BANEBERRY

by

Robert C. Shopland

This report contains a preliminary comparison of the relative ground motion of two NTS explosions, CYATHUS and BANEBERRY, which were of equal predicted yield and occurred at approximately the same epicenter.

Conventional short-period and long-period pendulum records from Queen Creek, Arizona (QC-AZ) at an epicentral distance of 618 km indicate that the ground amplitude of BANEBERRY on 18 December 1970 is approximately six times that of CYATHUS on 06 March 1970, as shown in figures 1 and 2. Both events are played back from magnetic tape at approximately equal system magnifications. Amplitude ratios between the two events are listed in table 1 for various phases.

To aid in determining the relative character of the two events, the short-period vertical pendulum outputs have been played back at approximately equal trace amplitude in figure 3. The Pn and Pg phases for the two events are almost identical on the short-period traces. However, it is noted that CYATHUS is recorded on the vertical trace (PZS) with less amplitude variation at periods exceeding approximately 1 second, particularly in the coda of Pg and in the coda of the surface group. The vertical long-period surface wave on trace PZL in figure 2 has a shorter period for CYATHUS than for BANEBERRY. However, the character of the long-period surface wave recorded on the P325L component of figure 3 shows little difference. Additional information will be available after a spectral analysis is run. Inertial data from the LRSM site at Houlton, Maine (HN-ME) and Tonto Forest Observatory (TFO) will be evaluated at a later date for the two events.

In contrast with the relatively large ground amplitudes recorded at QC-AZ from BANEBERRY, two LRSM portable strainmeter sites (YM-NV and QM-NV) at $\Delta \simeq 50$ km indicate about one-half as much earth strain from BANEBERRY as from CYATHUS, as shown in figure 4. Values of maximum quasi-static strain and the ratio of the strains for the two events are listed in table 2. Although it is reasonable to question the validity of the strain data on the basis that the amplitude of the signals are of the order of magnitude of the background noise, it is worthy of note that the strain steps correspond to the arrival time of the signal. Furthermore, the start of the strain step for BANEBERRY at sites YM-NV and QM-NV coincides with the arrival of the S wave. It is also interesting to note that the rise time for CYATHUS is about 1 minute in duration, whereas that of BANEBERRY is about 2 minutes.

A comparison of portable strain sites TI-NV and OB-NV is not possible because the two sites were not operating during one or the other of the events. Sites KP-NV and RH-NV were too distant to record either event. Figure 5 shows the location of the six portable strainmeter sites discussed above.

A high-frequency strain channel (0.1-50 Hz) was operated at the portable strain sites during BANEBERRY, but no high-frequency response data above 0.01 Hz was available during CYATHUS. However, a more effective comparison of future events will be possible when a system of 3-component inertial seismographs now being installed at sites RH-NV and YM-NV becomes operational.

Records from QC-AZ were furnished under Contract F33657-69-C-0121 and records from the portable strain sites under Contract F33657-70-C-0646.

Table 1. Ratio of maximum ground amplitude of BANEBERRY to CYATHUS for various phases

Phase	Amplitude Ratio (BANEBERRY/CYATHUS)			
	Short-Period		Long-Period	
	Vertical (PZS)	Horiz 325° (P325S)	Vertical (PZL)	Horiz 325° (P325L)
Pn	7.5	6.7	---	---
Pg	6.8	4.3	---	---
Sg-Lg	5.0	7.2	---	---
LR	7.0	4.8	5.8	4.0

Table 2. Ratio of maximum quasi-static strain for CYATHUS and BANEBERRY

Portable Strain Site	CYATHUS Strain	BANEBERRY Strain	BANEBERRY/CYATHUS Strain Ratio
QM-NV	1.5×10^{-9} e	0.65×10^{-9}	0.43 e
YM-NV	1.8×10^{-9} e	1.1×10^{-9}	0.61 c

e - extension

c - compression

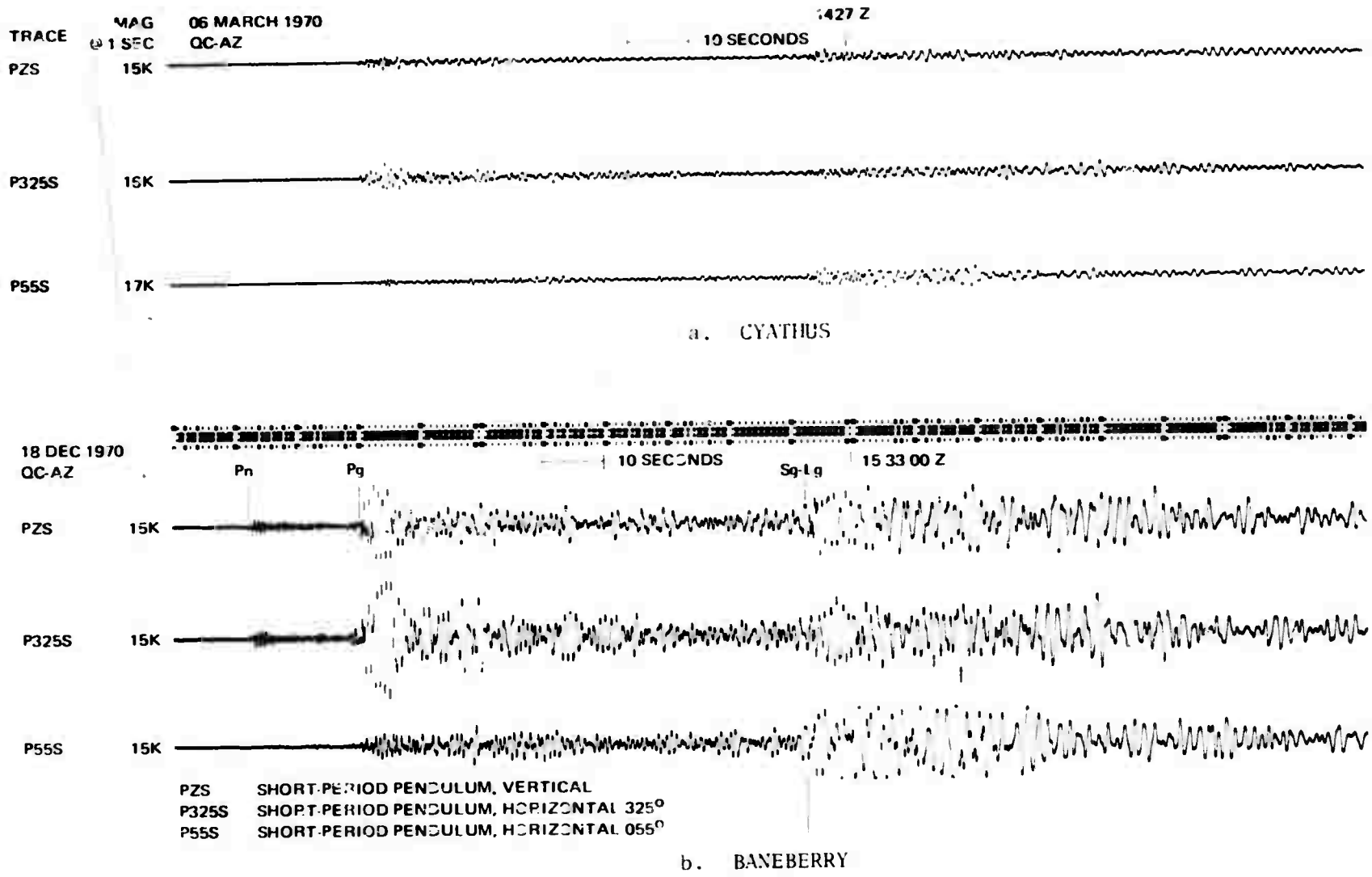

Figure 1. Magnetic tape playback of CYATHUS and BANEBERRY events recorded on 06 March and 18 December 1970, respectively, on 3-component short-period seismographs at Queen Creek, Arizona (QC-AZ)

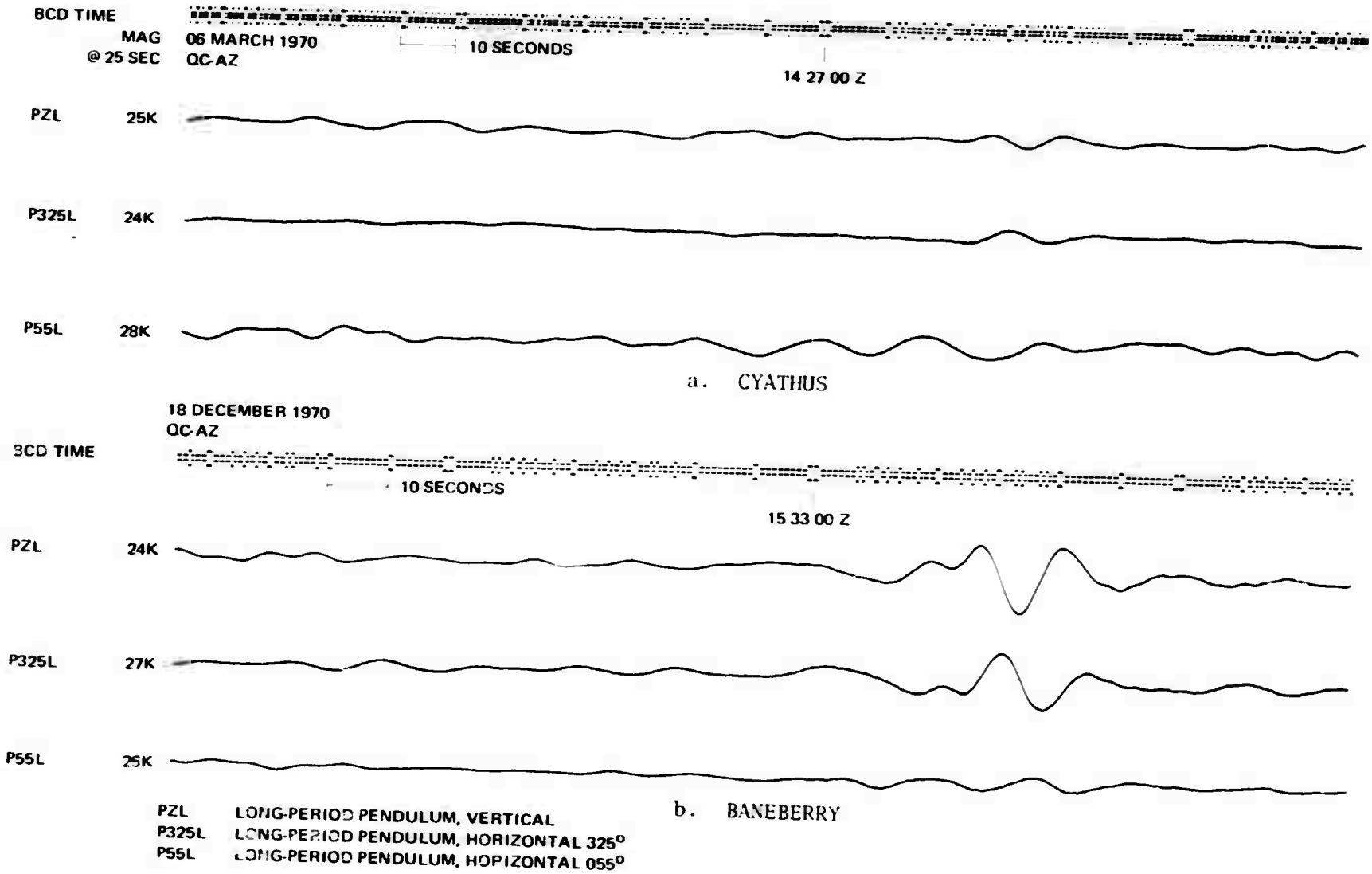

Figure 2. Magnetic tape playback of CYATHUS and BANEBERRY events recorded on 06 March and 18 December 1970, respectively, on 3-component long-period seismographs at Queen Creek, Arizona (QC-AZ)

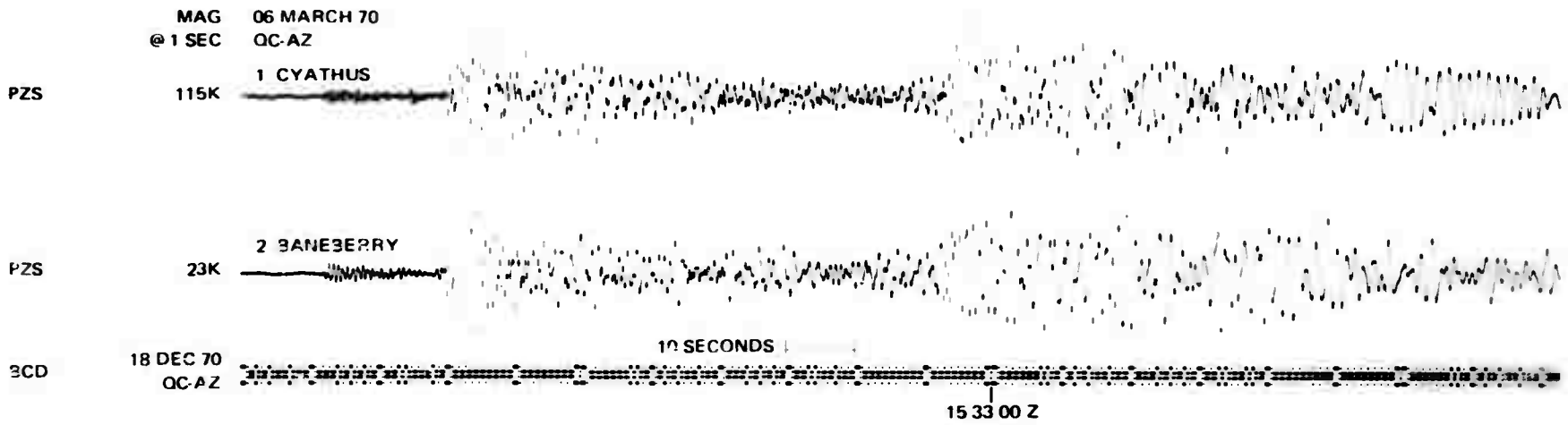

a. Short-period

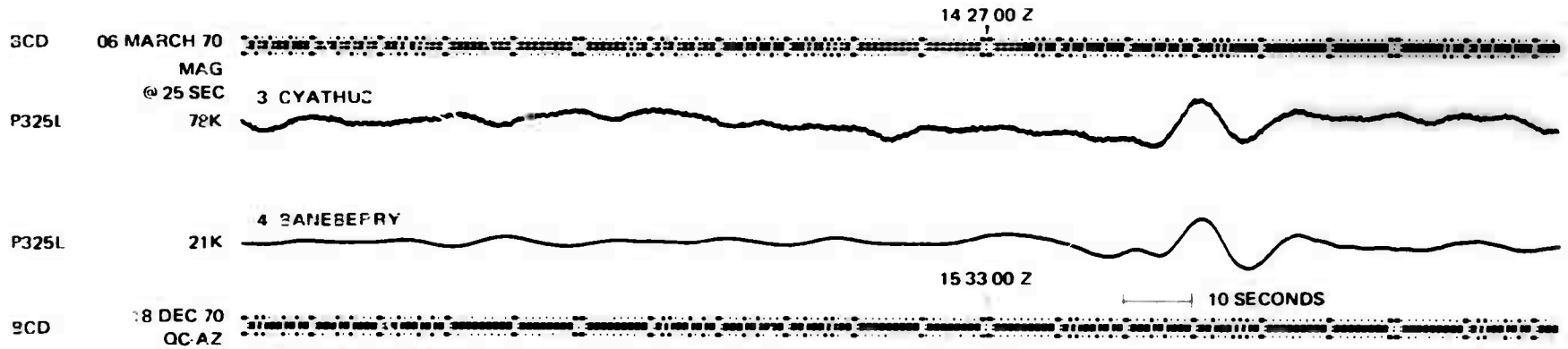

b. Long-period

Figure 3. Magnetic tape playback of CYATHUS and BANEBERRY events at approximately equal trace amplitude on the short-period vertical trace (PZS), trace 1 and 2, and on the long-period horizontal trace (P325L)

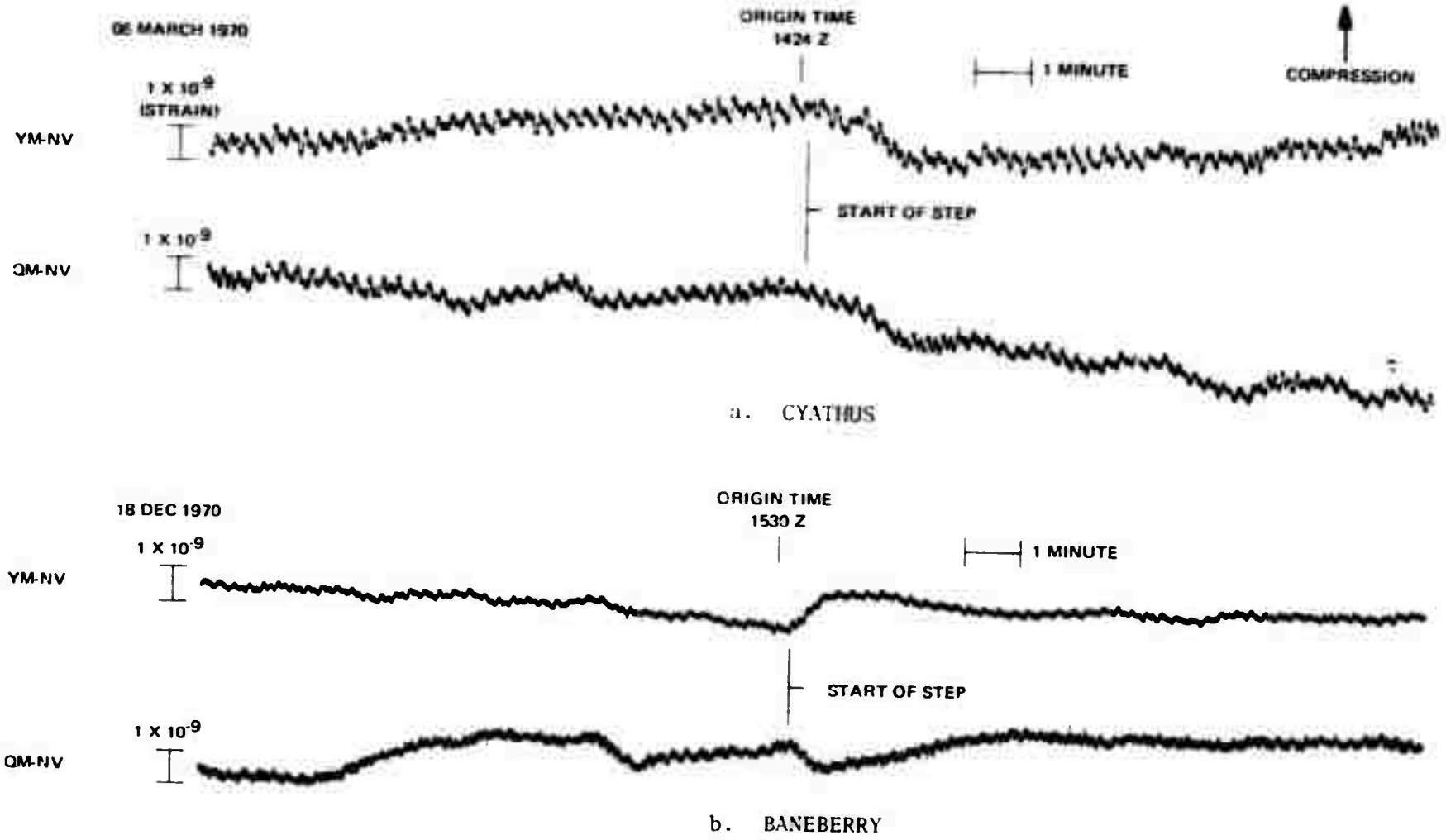

Figure 4. NTS explosions CYATHUS on 06 March 1970 and BANEBERRY on 18 December 1970 recorded at portable strain sites YM-NV (Δ = 49 km) and QM-NV (Δ = 46 km). The strain step from CYATHUS (1.6×10^{-9}) is larger than that from BANEBERRY (0.9×10^{-9}) and has a longer rise time

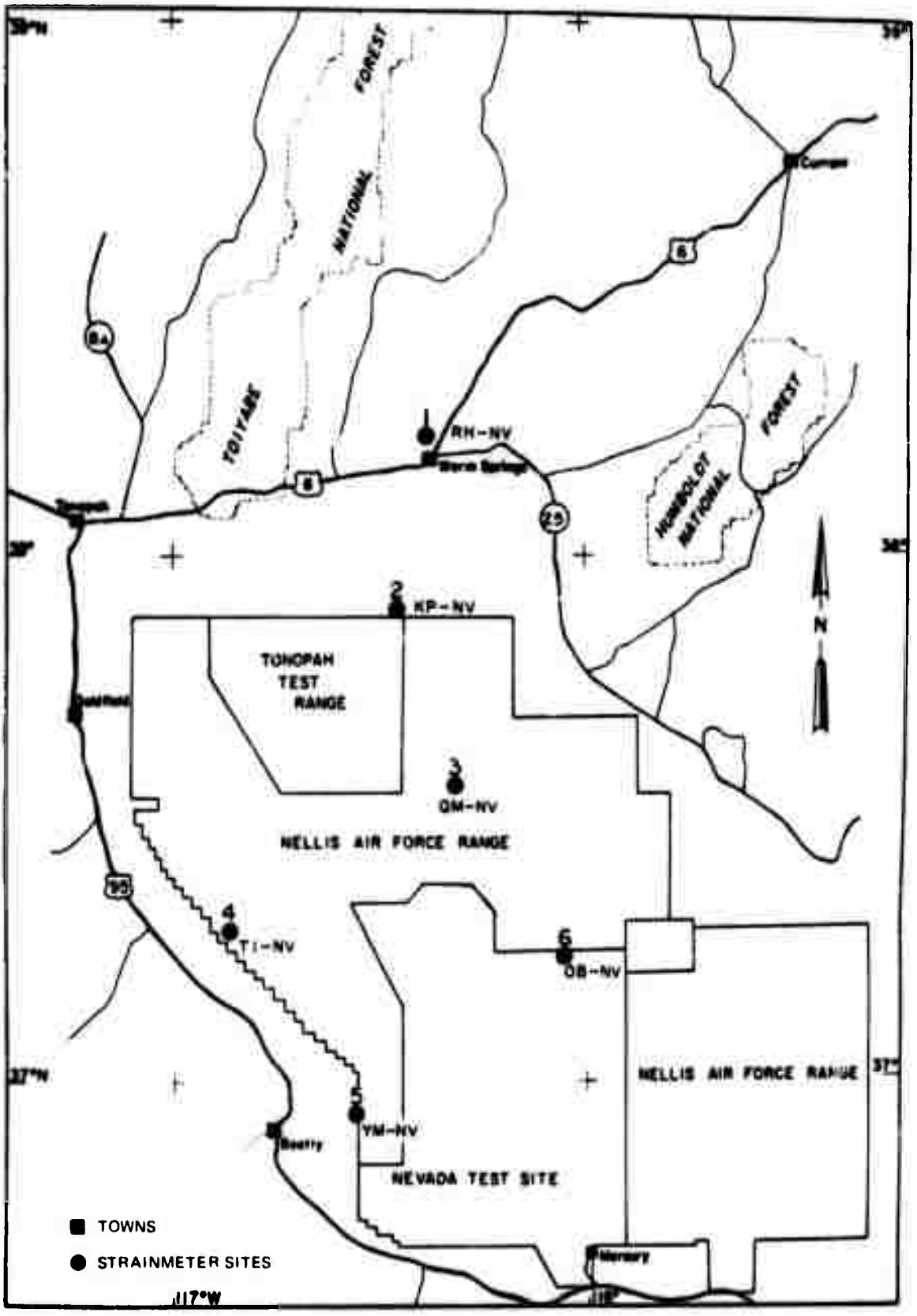

Figure 5. Location of strain sites

APPENDIX 3 to TECHNICAL REPORT NO. 71-20

PRELIMINARY NOTES ON THE SAN JOAQUIN VALLEY EARTHQUAKE OF 09 FEBRUARY 1971 FROM PORTABLE STRAIN RECORDS

19 May 1971

PRELIMINARY NOTES ON THE SAN JOAQUIN VALLEY EARTHQUAKE OF 09 FEBRUARY 1971 FROM PORTABLE STRAIN RECORDS

by

Robert C. Shopland

The following table summarizes the observations made to date on the San Joaquin Valley earthquake recorded on four of the six portable strain seismographs in Nevada. Listed are the amplitude of the strain step, the apparent velocity of the step, the apparent duration of the step, and remarks on signal condition and operational status.

Site	Strain step amplitude	Step velocity (km/sec)	Apparent duration principal step (minutes)	Remarks
QM-NV	6.4×10^{-9} e	5.06 km/sec	1.0	Good signal
YM-NV	6.5×10^{-9} C	5.03 km/sec	0.2	Good signal
TI-NV	2.9×10^{-9} C	(not timed yet)	-	Low signal-to-noise ratio
RI-NV	8.0×10^{-9} C	Cannot be measured	-	Recorded on Esterline-Angus paper record only
KP-NV	Out of range	-	-	Out of range
OB-NV	Inoperative	-	-	Inoperative

e - extension
C - compression

The information contained in records from QM-NV and YM-NV are of excellent quality. The system sensitivities were ideal for recording the San Joaquin earthquake. The low-gain wide-band trace contains valuable high-frequency information However, TI-NV is operated at a low sensitivity and, therefore, had a low signal-to-noise ratio. The signal at RH-NV, recorded on Esterline-Angus paper, contains only information on direction and amplitude of the strain step.

The velocity of the strain step for QM-NV and YM-NV are in close agreement and compare favorably to the average velocity 3.0 ±0.3 km/sec reported by Wideman and Major (BSSA, Dec. 1967). It is significant to note that the strain step is coincident with the arrival of the Sg phase. The step occurs 15 to 17 seconds after onset of the Sg phase and prior to the peaking of the long-period component.

The principal step associated with the Sg phase at YM-NV lasts 10 seconds longer than predicted by the filter response, and at QM-NV lasts 1 minute longer than predicted. It is possible that local strains are contributing to the duration of the step, or that the step is being triggered by more than one phase.

Additional analysis of the strain signal is required. The results will be reported in a final report on the portable strain operation.